MODIFICATION OF POLY(METHYL METHACRYLATE) SURFACES WITH AZOBENZENE GROUPS TO DEVELOP A PHOTORESPONSIVE SURFACE

by

Ashley Elizabeth Clarke

A thesis submitted to the Graduate Program in Chemical Engineering

in conformity with the requirements for the degree of

Master of Applied Science in Chemical Engineering

Queen's University

Kingston, Ontario, Canada

December, 2017

Abstract

Photoswitchable surfaces can be used to reversibly control surface wettability, adsorptivity, and protein adhesion to influence cell interactions at the surface. Control over protein adsorption and cell adhesion is useful in many applications, from cell culture scaffolds to drug delivery devices and improving the cell response to materials *in vivo*. Switchable properties can be attained by polymerizing light-responsive monomers or by modifying existing materials. This project investigates surface modification as a method of developing light-responsive poly(methyl methacrylate) (PMMA) surfaces and coatings of a copolymer of methyl methacrylate (MMA) and 2-aminoethyl methacrylate (AEM) (termed MMAcoAEM).

In this work, PMMA surfaces were functionalized with amine or carboxyl groups for azobenzene modification and cell-material interaction studies. PMMA was functionalized with hexamethylenediamine (HMD) or O,O'-bis(2-aminopropyl) propylene glycol-block-polyethylene glycol-block-polypropylene glycol (PPG-PEG-PPG) groups via aminolysis or functionalized with carboxyl groups via hydrolysis. Aminated PMMA was then modified with 4-(phenylazo)benzoic acid using a carbodiimide reaction. Surfaces were characterized using ninhydrin assays, titration, contact angle measurements, x-ray photoelectron spectroscopy (XPS), ultraviolet-visible (UV-VIS) spectroscopy and nuclear magnetic resonance spectroscopy (NMR).

The aminolysis reaction conditions from literature[1] were revised to improve the graft density, with up to 36.4 ± 7.0 nmol/cm^2 of HMD or 20.3 ± 2.9 nmol/cm^2 of PPG-PEG-PPG groups functionalized to PMMA. The copolymer MMAcoAEM contained 44.0 ± 2.2 nmol/cm^2 of amine

groups as a surface coating. Amine-functionalized PMMA or MMAcoAEM surfaces were modified with 20.5 ± 0.4 nmol/cm^2 (HMD), 11.2 ± 2.6 nmol/cm^2 (PPG-PEG-PPG), or 24.8 ± 4.4 nmol/cm^2 (MMAcoAEM) of 4-(phenylazo)benzoic acid. UV-VIS spectroscopy was used to confirm that azobenzene grafted to materials retained the ability to photoisomerize and interact with β-cyclodextrin (β-CD).

Functionalized PMMA was also used to study cell-material interactions with neutrophil-like HL-60 human promyelocytic leukemia cells activated with phorbol 12-myristate 13-acetate (PMA) to induce cell adhesion. AlamarBlue® assays and live/dead deoxyribonucleic acid (DNA) staining indicated that amine-modified surfaces contained the highest amount of extracellular DNA after incubation with HL-60s, believed to be extracellular traps (ETs). Future research aims to study the cell-material interactions with azobenzene-modified surfaces and further modify the surface using biomolecules conjugated to β-CD.

Co-Authorship

I hereby declare that this thesis contains material that is a result of joint research. HL-60 cell culture studies were completed by Chris Angelatos using materials jointly developed by Chris and the author. Chris independently collected both the alamarBlue® assay and DNA staining results under the supervision of Dr. Laura A. Wells. All written works pertaining to cell studies in this document were completed by the author.

I certify that all other contents of this thesis are my original work. All ideas and techniques of others included here are properly referenced in accordance with standard practices.

Ashley Clarke

Acknowledgements

I would like to express my sincerest gratitude to my supervisor Dr. Laura Wells for her guidance, support, and patience throughout my graduate work. Thank you for all your time and help with my research and thesis writing. Your dedication to your students is astounding and I am thankful to have had the pleasure to be a part of your research group.

I would like to thank Dr. Brian Amsden, Dr. Carlos Escobedo, and Dr. Louise Meunier for their insights and encouragement. I have taken classes with each of you while at Queen's and I am thankful to have such knowledgeable, friendly mentors in my thesis committee.

Finally, I would like to extend a heartfelt thanks to my friends and family for their endless support and confidence in me throughout my education.

This project was made possible using funding provided by the Natural Sciences and Engineering Research Council of Canada (NSERC) and facilities at Queen's University in Kingston, Ontario, Canada.

Table of Contents

List of Tables

List of Figures

List of Abbreviations

AEM	2-aminoethyl methacrylate
AFM	atomic force microscopy
Al	aluminum
ATRP	atom transfer radical polymerization
AZO	azobenzene
BPO	benzoyl peroxide
$CDCl_3$	deuterated chloroform
COOH	carboxyl
DNA	deoxyribonucleic acid
EDC	1-ethyl-3-(3-dimethylaminopropyl)carbodiimide
ET	extracellular trap
FBGC	foreign body giant cell
FBR	foreign body reaction
FBS	fetal bovine serum
HL-60	human promyelocytic leukemia cell line
HMD	hexamethylenediamine
IMDM	Iscove's modified Dulbecco's medium
IOL	intraocular lens
KHP	potassium hydrogen phthalate
M_w	Molecular weight
MAA	methacrylic acid

MES	2-(N-morpholino)ethanesulfonic acid
MMA	methyl methacrylate
MMAcoAEM	copolymer of methyl methacrylate and 2-aminoethyl methacrylate
NaOH	sodium hydroxide
NET	neutrophil extracellular trap
NH_2	amine
NHS	N-hydroxysuccinimide
NMR	nuclear magnetic resonance
PBS	phosphate-buffered saline
PCO	posterior capsule opacification
pH	power of hydrogen
pI	isoelectric point
PMA	phorbol 12-myristate 13-acetate
PMMA	poly(methyl methacrylate)
PPG-PEG-PPG	O,O'-bis(2-aminopropyl) propylene glycol-block-polyethylene glycol-block-polypropylene glycol
SAM	self-assembled monolayer
THF	tetrahydrofuran
UV	ultraviolet
VIS	visible
XPS	x-ray photoelectron spectroscopy

Chapter 1. Introduction

An important problem facing biomaterial development and implementation in the clinic is that foreign materials implanted into the body elicit a host response.[2] The host response depends on the mechanical and surface properties of a material and is ultimately responsible for biomaterial acceptance in the long-term.[3–5] Recent strategies to improve the cell response to biomaterials focus on mimicking extracellular matrix (ECM) components at the surface of biomaterials through the attachment of peptides[6,7] or deoxyribonucleic acid (DNA).[8,9] Molecules exhibiting anti-inflammatory,[10] anti-bacterial,[11] and anti-adhesive[12,13] characteristics have also been used to improve the host response. These specialized materials are commonly synthesized by conjugating the biomolecule to a monomer and reacting it into the main and/or side chain during polymerization. However, it is advantageous to coat the polymer or focus modifications at the surface so that the bulk properties of the polymer are minimally affected. Surface modifications can be used to adjust cell-material interactions and improve the host response to implants by altering surface wettability, topology, and charge.[14–16]

Biomaterials are typically designed to either enhance or inhibit cell interactions with the surface. For example, adhesion is desirable for orthopedic implant[17] and biodegradable scaffolding[18,19] integration into existing tissues. Comparatively, cell migration and adhesion is detrimental to the long-term function of artificial intraocular lenses (IOLs) implanted to improve vision by replacing cataracts. After implantation, the migration and proliferation of lens epithelial cells to the posterior segment of IOLs will gradually cause the lens to become opaque, resulting in posterior capsule opacification (PCO).[20,21] PCO can be treated by replacing the IOL or using laser

treatment to kill adhered cells, but either treatment can cause complications such as inflammation, infection, scarring, and damage to tissue surrounding the implant. The cell-material interactions at IOL surfaces *in vivo* have been improved by attaching heparin,[10] hyaluronic acid,[11] and chitosan[12] to the surface. Further development of these surfaces can be achieved using a method of tuning or modifying the surface properties to actively influence the adsorption of proteins and interaction with cells over time.

There are limitations when attempting to use static materials to interact with dynamic cellular environments. Over the course of the foreign body reaction, multiple cell types including neutrophils, macrophages, and fibroblasts may interact with a biomaterial surface. Additionally, cells may attach or migrate to biomaterials during wound healing or biomaterial integration into surrounding tissues. Although static materials can be well-suited for interactions with particular cell types, they cannot change over time to possess the surface properties best suited for each of these events. Responsive molecules have the potential to enhance interactions between biomaterials and cells by modulating hydrophobicity, adhesion, and adsorptivity via chemical or physical means.[22,23] Materials containing these molecules, termed "stimuli-responsive" materials, have been investigated for use as cell culture scaffolds,[24] diagnostic tools,[25,26] and drug delivery devices.[27,28] In regard to IOL development, attaching switchable responsive molecules to the IOL surface could be used to disrupt the attachment of cells and/or proteins from the lens and later recover the surface properties from before cell detachment.[29,30] Thus, it is beneficial to develop materials with a controllable method of altering surface properties. This thesis investigates surface modification as a method to attach responsive molecules to surfaces of poly(methyl methacrylate) (PMMA) and a copolymer of methyl methacrylate and 2-aminoethyl methacrylate

(MMAcoAEM). First PMMA is functionalized with either amine or carboxyl groups to promote reactivity, then amine-functionalized PMMA and MMAcoAEM surfaces are modified with the light-responsive molecule azobenzene. It is hypothesized that azobenzene can induce changes at the surface when irradiated.

Chapter 2. Literature review

2.1. Surface properties of biomaterials and their influence on protein adsorption

Both chemical and morphological properties will influence the interaction between a surface and the surrounding tissue. Cell-material contact *in vivo* is largely mediated by an aqueous layer of water molecules and a layer of adsorbed biomolecules at the surface.[16,31] Immediately after a biomaterial is implanted or incubated, a layer of proteins adsorbs to the surface to minimize free energy of the surface. The biomolecule layer consists primarily of proteins with the quantity and nature of proteins at the surface dependent on surface hydrophobicity, reactivity, charge, chain flexibility, and topology.[32,33] The underlying surface chemistry also plays a role in cell-material interaction,[31] however proteins are the center of intercellular interactions and signaling pathways and thus have an important impact on the inflammatory host response.

The structure of water molecules near a surface varies depending on the chemical nature of the surface.[34] A hydrophilic surface will strongly interact with surrounding water molecules causing a dense, disordered structure whereas water molecules surrounding a hydrophobic surface preferentially bond to themselves to form a more distinctive, less dense, ordered layer.[34] As a result, hydrophobic surfaces tend to adsorb proteins more quickly due to the availability of the surface for interactions and ease of displacement of surrounding water molecules.[34–36] Protein adsorption to a surface is influenced by protein size, abundancy, rigidity, and hydration layer structure.[37,38] The isoelectric point (pI) of a protein may also be used to determine its charge in relation to environmental pH and how the charged segments may interact with a charged surface. Proteins may change position or conformation to expose regions which bind strongly to the

polymer via intermolecular, ionic, or entropic (hydrophobic/hydrophilic) interactions as illustrated in Figure 2.1. Although locally abundant proteins will adsorb initially, in a short time proteins with a higher affinity for the surface may become more prominent, termed the Vroman effect.[33]

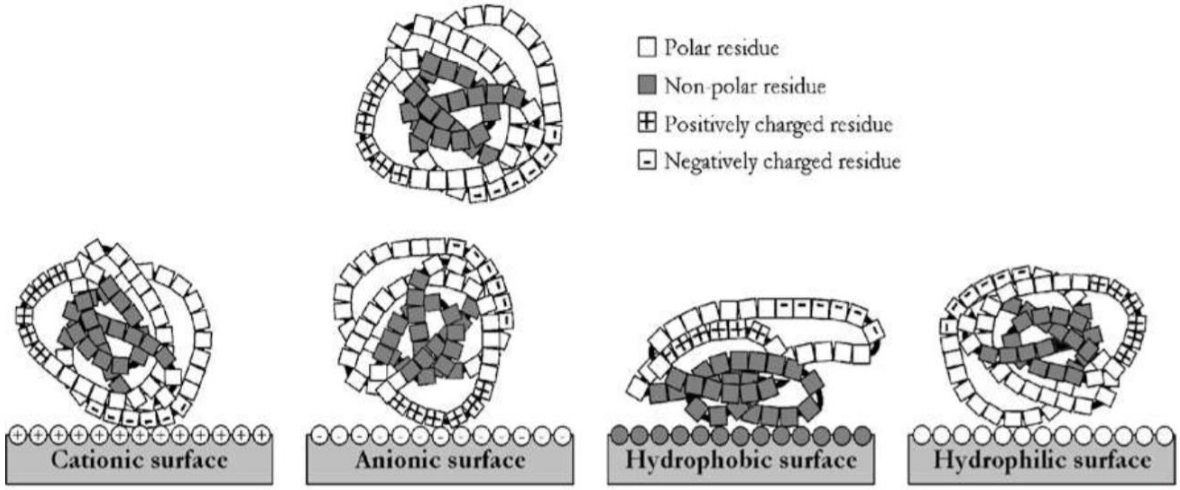

Figure 2.1. Charged and hydrophilic/hydrophobic protein interactions with a surface. Reprinted from Progress in Polymer Science, 32, Goddard *et al.*, Polymer surface modification for the attachment of bioactive compounds, 698-725, (2007), with permission from Elsevier.[39]

One challenge of using polymers for biomedical devices is that their properties are susceptible to change over time. With sufficient mobility, polymer chains can rearrange at the surface in reaction to the polarity of the immediate chemical environment. Flexible surface chains can lead to an increased penetration and content of water at the polymer surface, thought to increase the entropic gains associated with protein adsorption.[40] Additionally, flexible and hydrophobic polymer chains such as poly(ethylene glycol) (PEG) can be grafted to the surface to decrease protein adsorption.[13] Protein adhesion is a complex mixture of the aforementioned factors and is therefore difficult to predict.

2.2. Interactions between cells and materials and the foreign body response

One of the important aspects of biomaterial design is ensuring the material will be integrated into the host organism and will not invoke a chronic immune response. After a material is implanted into the body, a cascade of events termed the host response occurs which will result in either a foreign body response or healing.[3] During this process, various cell types migrate to the wound site to aid in the immune response, repair damaged tissues, remodel surrounding extracellular matrix, and interact with the implant (Figure 2.2).[4,5] As part of the immune response, neutrophils and macrophages are recruited to the site to interrogate the biomaterial and phagocytose foreign materials/microorganisms. Macrophages will undergo frustrated phagocytosis if the material is too large to be engulfed by the cell[41] and can aggregate to form larger foreign body giant cells (FBGCs) in an attempt to break down the material. An additional pathway for neutrophils to kill microorganisms is through the release of extracellular traps (ETs). Neutrophil extracellular traps (NETs) are fibers containing chromatin and antimicrobial proteins that can attach to and trap pathogens.[42,43] Recent literature has also identified the release of ETs from other immune cells.[44,45] If the immune cells are unable to breakdown the material, fibroblasts are recruited to the site to form a collagenous capsule around the implant, isolating it from the body and preventing the biomaterial from performing its intended function.[3] Surface properties and cell-material interactions have an important influence on whether a material is resorbed, encapsulated, or accepted by the host.[5]

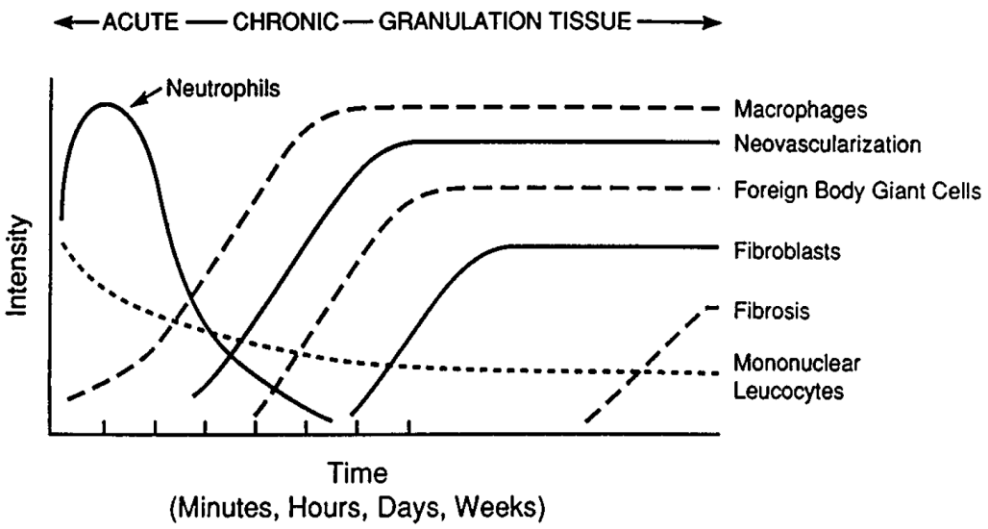

Figure 2.2: Timeline showing the changes in cell population surrounding an implant over time. Reproduced from James Anderson in Annual Review of Materials Research.[3]

Current research is focused on improving the cellular response to prolong device lifetime and minimize the need for correctional surgeries or new implants. For example, surface modification of acrylic and PMMA IOLs with heparin or hyaluronic acid has resulted in reduced post-operative inflammation and posterior capsule opacification (PCO) compared to unmodified materials.[10–12] However, macrophages have been shown to secrete more cytokines, chemokines, and enzymes on hydrophilic poly(2-hydroxyethyl methacrylate) IOLs than hydrophobic PMMA IOLs, which could affect the length and intensity of the inflammatory response *in vivo*.[46] The response of monocytic cells to materials *in vitro* may be investigated using a monocytic cell line such as the HL-60 human promyelocytic leukemia cell line. HL-60 cells continuously proliferate and may be differentiated to possess qualities of neutrophils and macrophages,[47–49] with well-established HL-60 differentiation protocols in literature using phorbol 12-myristate 13-acetate (PMA) to induce cell adherence and promote a neutrophil phenotype.[50–52]

2.3. Surface functionalization and modification of polymer surfaces

Polymers may be functionalized using physical, mechanical, or chemical means.[53] Physical methods such as lithography or exposure to electric field or ultraviolet (UV) light may be used to either modify the chemical surface or deposit a coating onto a material, but may be unstable or have a short lifetime.[22] Mechanical methods can be used to roughen the surface or create microstructures. Chemical methods such as adsorbing or covalently attaching molecules to surfaces are simple and are used to obtain stable changes in properties.[6,53–55]

Functional groups may be introduced into the main chain or side chains of polymers. Bulk functionalization can be achieved in solution or by adding groups during material synthesis. Comparatively, surface modifications via wet chemical methods, plasma treatment, ultraviolet (UV) irradiation, adsorption, coating, and self-assembled monolayers (SAMs) may be used to target the surface while minimizing changes to the bulk mechanical properties of a material. Within biomaterial research, carboxyl (COOH) and amine (NH_2) groups are commonly added to the surface to alter hydrophobicity or to promote reactivity. These groups can be conjugated to corresponding NH_2 or COOH groups on proteins or other biomolecules using carbodiimides such as 1-ethyl-3-(3-dimethylaminopropyl)carbodiimide (EDC) with reactive intermediate stabilization using N-hydroxysuccinimide (NHS).[6,56–58]

Wet chemical modifications rarely require specialized equipment and allow for modification of porous structures including microfluidic devices, unlike plasma and other energy-based treatments.[39] However, surface modification relies on polymer chain orientation and may result in different degrees of modifications for polymers with different molecular weights,

crystallinity, and/or tacticity.[39] One wet chemical method, aminolysis, has been widely used to functionalize polymers with amine groups.[1,7,19] Copper-catalyzed click chemistry[59] and reduction with lithium aluminum hydride[26] have also been used and can attain higher amine graft densities, however there is a possibility that these chemical can persist in the material and harm cells downstream. Similarly, acid- or base-catalyzed hydrolysis is commonly used to convert surface ester groups to carboxylic acids and is advantageous over physical functionalization methods, such as plasma or UV-treatment, as it is more selective towards COOH groups.[60–62]

2.4. Poly(methyl methacrylate) (PMMA) uses as a biomaterial

Poly (methyl methacrylate) (PMMA) is a synthetic, hydrophobic thermoplastic consisting of repeating units of a methyl methacrylate (MMA) monomer (Figure 2.3). The polymer is lightweight, resistant to scratches and environmental deteriorations PMMA is also optically transparent (refractive index 1.49) and thus has been used for lab-on-chip devices[62,63] and ocular devices including IOLs and contact lenses.[64,65]

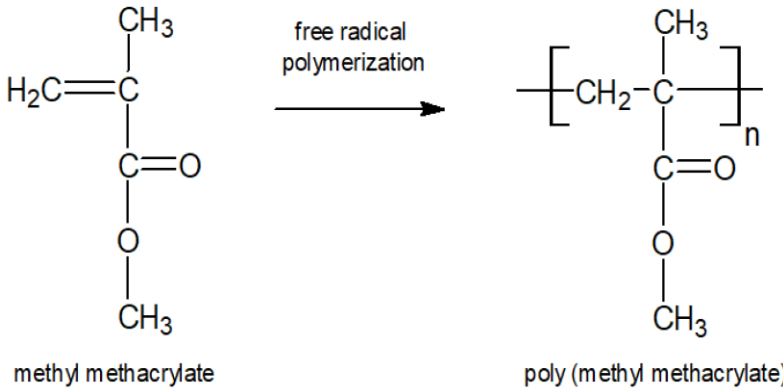

Figure 2.3: Monomer methyl methacrylate (MMA) and common initiators used for polymerization into poly(methyl methacrylate) (PMMA).

Both modified PMMA and PMMA copolymers have been investigated as biomaterials.[66–70] As a rigid hydrophobic material, PMMA has a lower surface roughness than other more hydrophilic acrylics and has demonstrated lower protein adsorption than silicone and hydroxyethyl methacrylate hydrogel IOLs.[20,71] Copolymers of PMMA exhibiting block hydrophilic and hydrophobic characteristics can also result in less cell attachment and proliferation *in vivo* than purely hydrophilic or hydrophobic IOLs.[21,64] Additional improvements to the host response to PMMA have been achieved using functional groups[65] or biomolecules such as proteins[7] or DNA.[8,72]

2.5. Stimuli-responsive molecules can improve interactions between biomaterials and their surroundings

Materials capable of a swift change in properties in response to a physical (light, temperature, magnetic) or chemical (pH, enzymatic) stimulus are known as "stimuli-responsive" or "smart" materials. Currently, stimuli-responsive polymers are being used to develop drug delivery, cell culture, and diagnostic tools due to their versatility and ability to respond to their surrounding environment. Combinations of modification methods may also be used to obtain multi-active surfaces capable of responding to more than one type stimulus.[22] Chemical stimuli can be used to induce highly stable property changes, however physical stimuli are useful in applications requiring a reversible change or where the system is difficult to access or complex in nature – such as with biomaterials.

Temperature-, pH-, and light-responsive materials are the most widely-studied for biomaterials as they are easy to stimulate, well-controlled, and often exhibit reversible changes. In

a cellular environment, direct changes to pH or temperature will consequently affect the cellular environment and may be difficult or impractical to alter *in vivo*. In this regard, light-responsive materials are advantageous as they can be used to manipulate properties externally. The wavelength and intensity of irradiation may have to be limited to prevent excessive damage to cells, and light is not practical to activate materials beneath opaque tissues, limiting its applications. However, the affordable, easily controllable, economic, and physical nature of light makes it a sensible stimulus for use in a biological environment.

Photochromic molecules can be used to develop light-responsive materials. These molecules change structure after absorbing ultraviolet (UV) or visible (VIS) light of a particular energy and can be synthesized into monomers,[69,73,74] coated onto a surface,[75,76] self-assembled,[77,78] or grafted to polymers.[27,79] A selection of photochromic molecules are included in Figure 2.4 below. Spiropyrans, spiroxamines, and fulgides exhibit intramolecular bond breaking and/or forming when stimulated, while azobenzenes exhibit a reversible photoisomerization between the *trans*- and *cis*- states. Diarylethenes can exhibit either of these structural changes. Azobenzenes and some diarylethenes (e.g. stilbene) also have the ability to form an inclusion complex with the conical sugar molecule cyclodextrin when in the *trans*- form, providing an additional tool for customization of properties (discussed in section 2.6.1).[80,81]

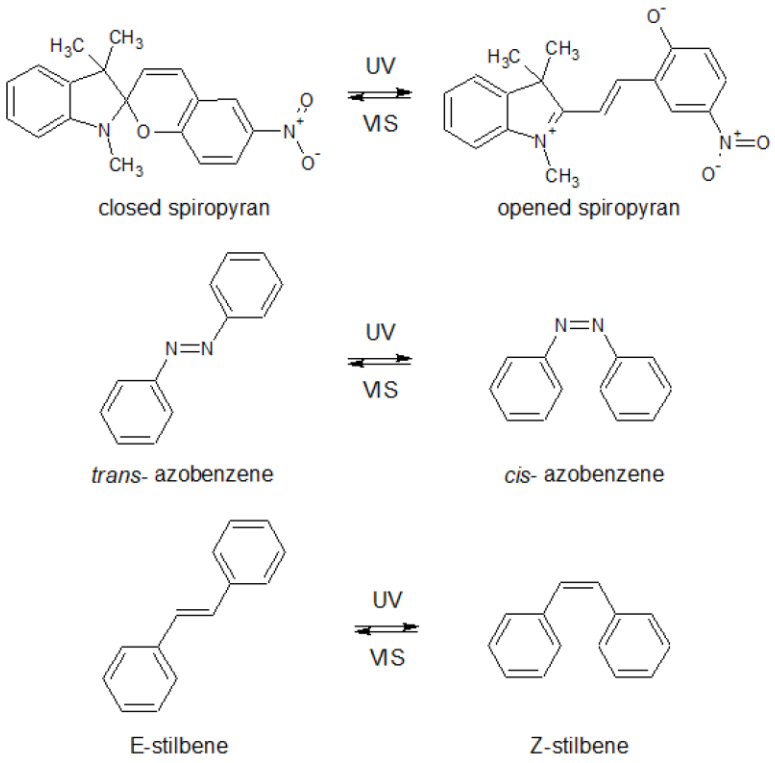

Figure 2.4: Changes in structure of common photochromic molecules after ultraviolet (UV) or visible (VIS) irradiation. Adapted from Reference 23 with permission of The Royal Society of Chemistry.[23]

2.6. Azobenzene as a photoswitchable molecule for biomaterial applications

Azobenzene has a widely studied and well-controlled photoisomerization. Azobenzene transitions from *trans*- to *cis*- when irradiated with 320 nm light and reversibly isomerizes (*cis*- to *trans*-) when irradiated with 440 nm light or heated to 60 °C (thermal relaxation). The photoisomerization wavelength and efficiency minimally change with the size, position, number, and type of substituents on the aromatic rings of azobenzene.[82,83] The isomerization is also effected by solvent and greatly influenced by packing density of the chromophore.[84–88] Azobenzene is highly hydrophobic and may only dissolve in water to a $5.5x10^{-4}$ – 0.1 mM in the *trans*-conformation, however this is the main driving force for its strong host-guest interactions with cyclodextrins.[86,89]

Azobenzene has traditionally been used as a dye for textiles, but recent literature has focused on its responsive properties to develop optically active materials.[27,74,90,91] The most common method of azobenzene distribution within a material is to combine the moiety with a monomer for polymerization. Azobenzene-containing monomers have been synthesized for applications in liquid-crystal polymers,[85,88,92,93] shape-changing polymers,[91,94] polymer networks,[95,96] and polymer brushes.[74,97,98] A range of methacrylate-containing photoresponsive polymers have been synthesized using the above methods.[66,69,79,99,100] Physical properties of said polymers including thermal stability, chain anisotropy, wettability, and photoisomerization behavior are manipulated by varying the location and quantity of azobenzene groups in the material.[74]

Self-assembly and chromophore adsorption onto polymers have also been explored to add photoresponsive groups to the surface (Figure 2.5). As previously stated, surface modification is advantageous as it may be used to target modification at the surface, retain native thermal and mechanical properties of the polymer, and develop more complex materials. Self-assembled monolayers (SAMs) consisting of azobenzene-terminated alkanethiols have been developed for applications in optical memory storage and as sensors.[101,102] Using similar molecular dynamics, self-assembling polymer micelles containing azobenzene have also been studied.[78,103] This method provides highly arranged photoresponsive surfaces, however the packing density must be controlled as it greatly impacts the photoisomerization yield and material functionality.[77,101,104] Minimal research has explored the use of wet chemical modifications to add photoresponsive properties to materials.

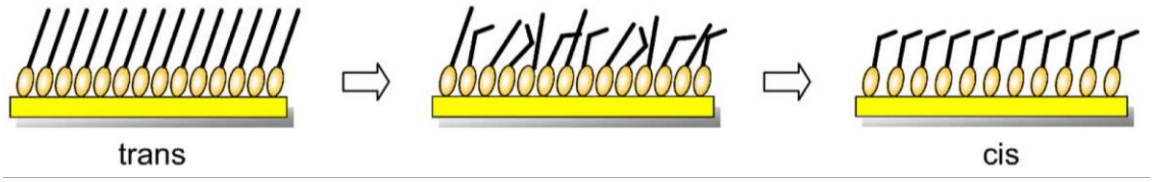

Figure 2.5: Azobenzene self-assembled monolayers associate to the surface via intermolecular interactions between the head group (egg. alkanethiol) and the surface. Reprinted from Applied Surface Science, 228, Micheletto *et al.*, Real time observation of trans–cis isomerization on azobenzene SAM induced by optical near field enhancement, 265-270, (2004), with permission from Elsevier.[101]

2.6.1. Host-guest complexation between azobenzene and cyclodextrin

β-cyclodextrin (β-CD) is a conical molecule made up of linked α-D-glucopyranoside units forming a hydrophobic interior and hydrophilic exterior, allowing encapsulation of hydrophobic molecules in aqueous media. Cyclodextrin has been used to encapsulate hydrophobic drugs in solution[105] and to form complexes with polymers[106,107] and photoresponsive molecules.[81,106] The strength of the host-guest interaction depends on the hydrophobicity of the guest molecule and the size of the cyclodextrin ring. The *trans*-form of azobenzene complexes with both α-cyclodextrin and β-CD (6 and 7 repeating units), while the *cis*-form can associate with β-CD but has a less favourable interaction than the *trans*- isomer (Figure 2.6).[108–111]

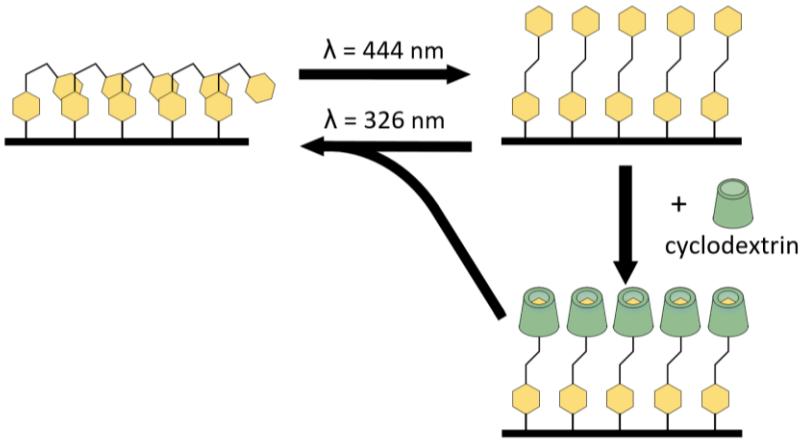

Figure 2.6: Photoisomerization of azobenzene with photoisomerization wavelengths (λ) for 4-(phenylazo)benzoic acid. Cyclodextrin has strong interaction with azobenzene in the *trans*- form so selective irradiation of the surface can result in cyclodextrin patterning on the surface.

These interactions have been used to obtain reversible systems closed with *trans*-azobenzene and opened by irradiating the molecules to the *cis*- causing dissociation from cyclodextrin.[28,109] This property has been applied to the self-assembly of polymers and polymer structures[108–110,112–114] and for the controlled release of hydrophobic molecules from nanoparticles and micelles for drug delivery applications.[27,28,115] Another application could be used to reversibly add peptides, nucleic acids, or biomolecules modified with β-CD to surfaces containing azobenzene to alter the cell response to the surface.

2.7. Outline of thesis and research objectives

The hypothesis of this thesis is that wet chemical grafting of azobenzene to PMMA surfaces will generate a photo-controllable, responsive polymer that will reversibly bind to β-CD. In future studies, this would allow for disruption of cell culture through surface property manipulation or for reversibly adding biomolecules to the surface via β-CD complexation with azobenzene. Although grafting is not as prominently studied in the literature, it is hypothesized this method will allow for easy removal of reaction byproducts, may be applied to post-processed materials, allows for retention of native bulk properties, and has potential to be applied to materials other than PMMA. Surface modifications to PMMA disks and coated coverslips utilized diamine spacers to functionalize the surface prior to azobenzene modifications while bulk modifications were performed on a copolymer of methyl methacrylate and 2-amino ethyl methacrylate (MMAcoAEM).

In this work, wet chemical modifications are performed on PMMA to produce surfaces which are photoresponsive. In order to modify the surface with azobenzene, PMMA is first

aminated using an adaptation of the method from Fixe et al.[1] The amine and azobenzene surfaces are characterized using ninhydrin assays, contact angle, x-ray photoelectron spectroscopy (XPS), and absorbance in the ultraviolet/visible (UV-VIS) spectrum. An additional functionalization was performed on PMMA to add carboxyl groups at the surface. Amine and carboxyl functionalized PMMA were also used to culture cells to investigate the cell response to the surfaces. Smoothed PMMA was characterized using atomic force microscopy (AFM) prior to cell studies and alamarBlue® assays were used to infer cell viability. Experiments are summarized in Figure 2.7 and Figure 2.8 with the objectives of this work listed below.

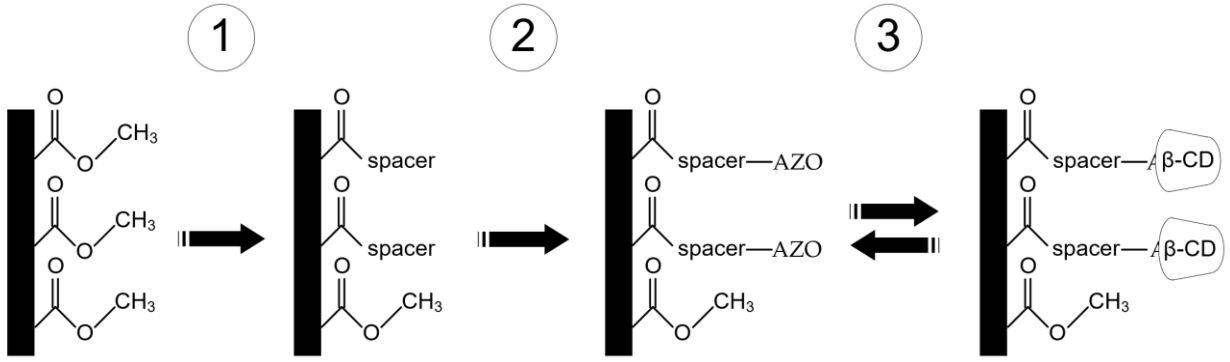

Figure 2.7: Poly(methyl methacrylate) (PMMA) modification pathway where diamine-terminated spacers were added to PMMA to increase the reactivity of the surface (1), 4-(phenylazo)benzoic acid (AZO) was grafted to the amine spacer (2), and surfaces were incubated in β-cyclodextrin (β-CD) (3).

Objective 1. Functionalize PMMA with carboxyl and amine groups to increase reactivity of the polymer: Carboxyl groups will be added via hydrolysis while amine groups added via aminolysis with diamine terminated spacer molecules. Functionalization will be focused at the surface and reacted surfaces compared to unfunctionalized controls for quantification. Surface properties will be investigated including cell interactions of HL-60 cells with the functionalized materials.

Objective 2. Modify amine-containing PMMA with carboxylated-azobenzene via carbodiimide chemistry: This will be investigated first using the amine-functionalized PMMA from Objective 1 and secondly using a copolymer of MMA and the monomer 2-aminoethyl methacrylate (AEM). The materials will be quantified and any changes to surface properties investigated.

Objective 3. Investigate the photoisomerization of azobenzene attached to surfaces: Ultraviolet-visible (UV-VIS) spectroscopy will be used to monitor the photoisomerization of azobenzene grafted to polymers and compared to azobenzene in solution. In addition, interactions between β-CD and azobenzene-modified surfaces were studied using contact angle and UV-VIS spectroscopy.

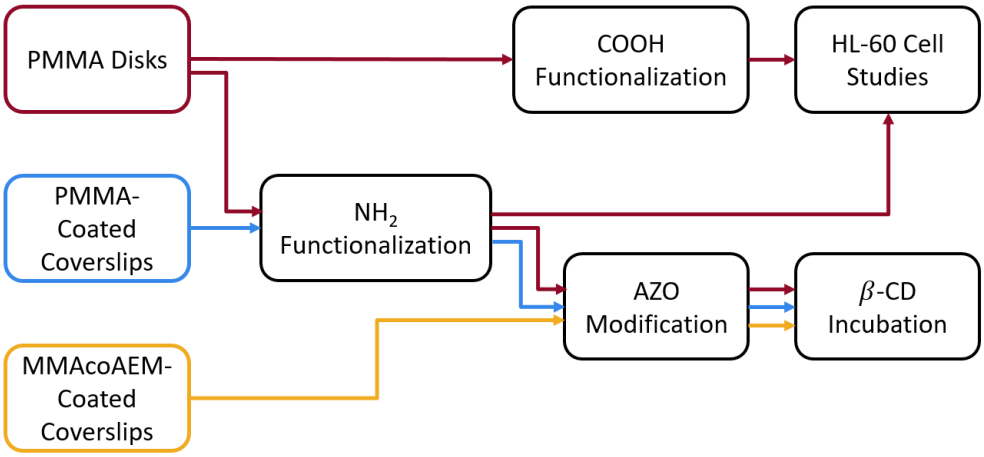

Figure 2.8: Experiment flow of poly(methyl methacrylate) (PMMA) and the copolymer methyl methacrylate-co-2-aminoethyl methacrylate (MMAcoAEM) functionalization, modification, and human promyelocytic leukemia (HL-60) cell studies. PMMA was functionalized with amine (NH_2) or carboxyl (COOH) groups and both polymers modified with 4-(phenylazo)benzoic acid (AZO) and β-cyclodextrin (β-CD) groups.

Chapter 3. Research methodology

3.1. Materials and reagents

Poly(methyl methacrylate) (PMMA), methyl methacrylate (MMA), 2-aminoethyl methacrylate hydrochloride (AEM), benzoyl peroxide (BPO), hexamethylenediamine (HMD), O,O'-bis(2-aminopropyl) propylene glycol-block-polyethylene glycol-block-polypropylene glycol ($PPG_{1.8}$-PEG_9-$PPG_{1.8}$), 4-(phenylazo)benzoic acid, and β-cyclodextrin (β-CD) were purchased from Sigma Aldrich (Oakville, ON, CA). PMMA disks from Tap Plastics (Stockton, CA, USA) were used in the initial surface functionalization while 12 mm round glass coverslips from VWR International were used for PMMA coatings. Trione® ninhydrin reagent from Pickering Laboratories (Mountain View, CA, USA) was obtained through Thermo Fisher Scientific. For cell culture, Iscove's Modified Dulbecco's Medium was obtained from the American Type Culture Collection (ATCC, Burlington, ON, CA) and supplemented with 20% fetal bovine serum from Wisent Inc. (Saint-Jean-Baptiste, QC, CA) and 1% penicillin/streptomycin solution from GE Healthcare/Life Sciences (Mississauga, ON, CA). Gibco phosphate buffered saline (PBS), alamarBlue® reagent, NucBlue® Live Cell ReadyProbes® Reagent, SYTOX® Green Nucleic Acid Stain, formalin (4 % formaldehyde), and anti-fade were purchased from Thermo Fisher Scientific and phorbol 12-myristate 13-acetate (PMA) purchased from Sigma Aldrich (Oakville, ON, CA). All water was filtered using a Millipore system (Millipore (Canada) Ltd, Etobicoke, ON, CA) and all other chemicals used as received from Sigma-Aldrich (Oakville, ON, CA).

3.2. Surface functionalization of PMMA with amine and carboxyl groups

3.2.1. Preparing PMMA disks and PMMA-coated coverslips for functionalization

Poly (methyl methacrylate) surfaces were prepared by smoothing PMMA disks or coating 12 mm circular glass coverslips with a thin layer of PMMA via solution-casting. PMMA disks were smoothed by covering the top surface of 2 mm thick PMMA disks in 100 μL of chloroform and air-drying them for 24 h covered in a glass petri dish followed by 48 h uncovered. For coating the glass coverslips, 20 mg/mL of PMMA in chloroform was prepared 24 h in advance to allow the PMMA to fully dissolve. Coated coverslips were prepared by pipetting 80 μL of 20 mg/mL PMMA in chloroform onto coverslips and drying for 24 h while covered in a glass petri dish followed by 48 h uncovered. The disks and coated coverslips were further dried for 48 h in a vacuum oven at 30 °C.

3.2.2. Amine functionalization of PMMA disks and PMMA-coated coverslips

Surfaces were aminated with a short or long diamine spacer using an adaption of the method developed by Fixe et al.[1] In this work, hexamethylenediamine (HMD, molecular weight (M_w) = 116.21 g/mol) or O,O'-bis(2-aminopropyl) propylene glycol-block-polyethylene glycol-block-polypropylene glycol (PPG-PEG-PPG, approximate M_w = 600 g/mol) was dissolved to 20 v/v% in a sodium tetraborate buffer solution at a pH of 11.5 or 12.5 for reaction (Figure 3.1). The buffer was prepared using 1 N sodium hydroxide (NaOH) to adjust the pH of a 0.1 M sodium tetraborate and 0.15 M sodium chloride solution. After cleaning the surfaces once with 5 mL isopropanol and twice with 5 mL Millipore water, each sample was incubated in 2 mL of 0.003 mol of HMD or 0.0007 mol of PPG-PEG-PPG in sodium tetraborate buffer solution. The reaction occurred under stirring at room temperature for 2 – 48 h on a rotating plate at 60 rpm,

then samples were rinsed with excess water and air-dried. The number of amine groups at the surface were quantified using a ninhydrin assay.

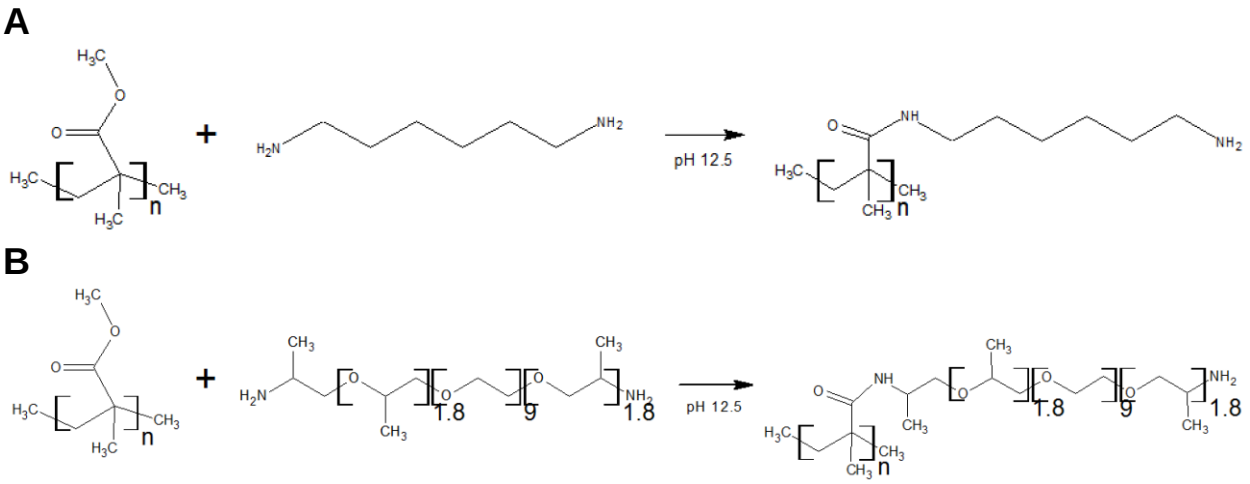

Figure 3.1: Reaction mechanism for aminolysis reaction of PMMA surfaces with HMD (A) or PPG-PEG-PPG (B) diamine spacers.

3.2.2.1. Amine functionalization was quantified using a ninhydrin assay

The ninhydrin assay is a widely used chromatographic method to quantify primary and secondary amines. The dye assay was developed for the analysis of amino acids,[116] and is used today to analyze a wide variety of amine-containing compounds. Ninhydrin oxidizes compounds with primary amines to an aldehyde with one less carbon atom while producing carbon dioxide and ammonia. The reduced ninhydrin (hydrindantin) and ammonia then react to form Ruhemann's purple, with a maximum absorbance at 570 nm. The amine functionalizations were quantified using the Trione® ninhydrin reagent, composed of sulfolane (25-50%), lithium acetate buffer (10-25%), ninhydrin hydrate (≤ 2.5%), hydrindantin (≤ 1.0%), and distilled water (25-50%).

Each functionalized disk or coated coverslip was incubated in 1 mL of deionized water overnight. To each sample, 0.5 mL of Trione® Ninhydrin Reagent was added then samples were

placed in a 100 °C oil bath. After 10 minutes, the samples were removed and cooled to room temperature while standards of glycine in deionized water ranging from 0 M to $4x10^{-4}$ M were prepared (see sample standard curve in Figure 3.2). The absorbance of each ninhydrin sample was measured at 570 nm using a Perkin Elmer Enspire Multimode Plate Reader and the amine concentration calculated using a glycine standard curve. The number of amine groups added to the surface is reported as the difference between the amine concentrations of functionalized and unfunctionalized (control) PMMA samples.

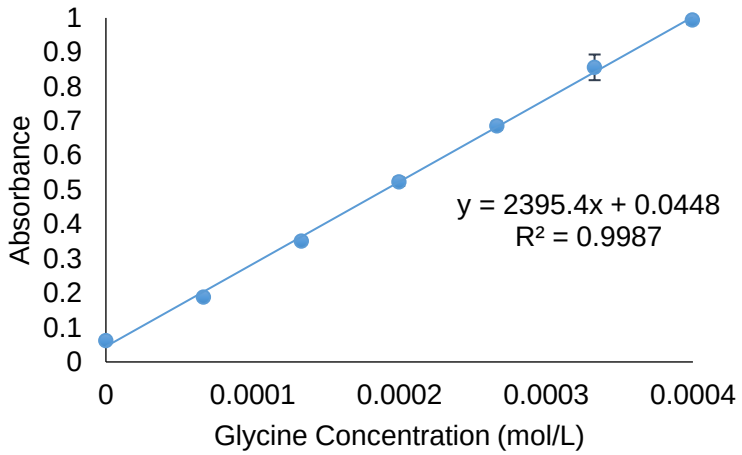

Figure 3.2: A representative standard curve of glycine in Millipore water measured at 570 nm used to calculate the amine concentration of functionalized samples.

3.2.3. Carboxyl functionalization of PMMA disks

Smoothed PMMA disks were functionalized with carboxyl groups using an adaption of the method developed by Patel et al.[60] Each disk was rinsed with 5 mL isopropanol, 5 mL of Millipore water, then added to a vial containing 2.5 mL of a 1:1 volume ratio of methanol and either 1 N or 6 N NaOH solution. After reacting for 2 – 6 h at 60 °C, each disk was rinsed with 5 mL of Millipore water and air-dried for 24 h in a well plate. The carboxyl groups were quantified using titrations, treating reacted surfaces as a copolymer of methyl methacrylate (MMA) and methacrylic acid (MAA) (equivalent to carboxylated MMA).

3.2.3.1. Carboxyl functionalization was quantified using titrations

Titration is a method of determining the concentration of acid or base in a sample via adding a complementary acid/base and monitoring pH through the neutralization reaction. The amount of carboxyl groups at the surface of functionalized PMMA was determined by back titration of NaOH incubated with the disks. Three vials of functionalized PMMA disks, unfunctionalized PMMA disks, and controls containing no disk were used for each trial. Each disk was incubated in 10 mL of an 8.33 mM NaOH solution overnight. Separate vials contained 2 mL of 8.44 mM potassium hydrogen phthalate (KHP) solution along with one drop of phenolphthalein. To determine the number of carboxyl groups that had been neutralized during the incubation, NaOH solutions were slowly pipetted into KHP vials until a colour change was observed. The final NaOH concentration was calculated by dividing the moles of KHP titrated against by the volume of NaOH titrated. The concentration of NaOH from incubated samples was compared to the control concentration and the number of carboxyl groups on functionalized surfaces reported as the difference between functionalized and unfunctionalized PMMA disks.

3.3. Copolymerization to generate an amine-functionalized polymer

A copolymer of 2-aminoethyl methacrylate (AEM) and methyl methacrylate (MMA) was prepared via free radical polymerization using benzoyl peroxide (BPO) as initiator. Monomers were measured based on a theoretical 60 mol% MMA and 40 mol% AEM copolymer (10 wt% BPO) termed MMAcoAEM. First, 0.32 mL of MMA, 0.331 g of AEM and 0.048 g of BPO were added to a round bottom flask with 20 mL of Millipore water. Nitrogen gas was bubbled through the mixture for 5 minutes then the flask was submerged in a 70 °C pre-heated oil bath under reflux and stirred for 2 h. After the reaction, the mixture was cooled to room temperature and the excess

solution decanted while the precipitated copolymer was dissolved into ~ 20 mL of tetrahydrofuran (THF). The polymer/THF solution was slowly added to a 500 mL beaker of Millipore water and the copolymer precipitate extracted into a separate container to be dried. Nuclear magnetic resonance (NMR) spectroscopy and ninhydrin assays were used to determine the purity and final concentration of amine groups in the copolymer. The copolymer was prepared in bulk and coated onto glass coverslips by dispensing 80 μL of 50 mg/mL MMAcoAEM in chloroform onto each coverslip and evaporating the solvent for 24 h while covered in a glass petri dish followed by 48 h uncovered. The coated coverslips were further dried for 48 h under vacuum in a vacuum oven at 30 °C.

3.3.1. Nuclear magnetic resonance spectroscopy to investigate copolymer structure

In this work, nuclear magnetic resonance (NMR) is used to verify the molecular structure and assess the purity of MMAcoAEM after polymerization. NMR operates on the principle that nuclei with angular momentum also have a small magnetic moment. Applying an external magnetic field to these nuclei introduces the potential for a transition to a higher energy state from a lower energy state. When returning to the lower energy state, energy is emitted and measured to develop an NMR spectrum. Information may be gained from the number of peaks, chemical shift, peak area, and splitting behaviour in a spectrum. Chemical shifts and splitting behaviour may also be compared to libraries containing spectra for known compounds and impurities.[117]

The structure of MMAcoAEM was assessed by comparing the O-CH_3 peak from the proton (^{1}H) NMR spectrum of PMMA and the O-CH_2-CH_2-NH_2 peaks from the ^{1}H NMR spectrum

of MMAcoAEM. Proton NMR was collected using a Bruker AVANCE 300 MHz spectrometer at room temperature with polymers prepared at a concentration of 20 mg/mL using deuterated chloroform ($CDCl_3$) as solvent. As PMMA is atactic and not all repeating units are chemically equivalent, some peaks were not fully resolved, leading to difficulties when assigning peaks.[118] Spectra were analyzed using Bruker TopSpin (Milton, Ontario, CA) and are reported using parts per million (ppm).

3.4. Azobenzene modification of PMMA disks, PMMA-coated coverslips, and copolymer MMAcoAEM

Aminated PMMA and MMAcoAEM-coated coverslips were modified using the same procedure. Approximately two azobenzene groups were added to the reaction solution for each amine detected by the ninhydrin assay. Each disk or coverslip was incubated in 1 mL of 2-(N-morpholino)ethanesulfonic acid (MES) buffer (pH 6) containing 0.23 mg of 4-(phenylazo)benzoic acid, 0.96 mg of 1-ethyl-3-(3-dimethylaminopropyl)carbodiimide (EDC), and 0.58 mg of N-hydroxysuccinimide (NHS) (see Figure 3.3). The buffer was prepared using 1 N sodium hydroxide (NaOH) to adjust the pH of a 0.1 M MES and 0.5 M sodium chloride solution. After reacting for 24 h at room temperature in the dark, the disks and coverslips were rinsed with excess water and stored in a fresh microplate to dry. Azobenzene modifications were analyzed using ninhydrin assays, contact angles, and XPS.

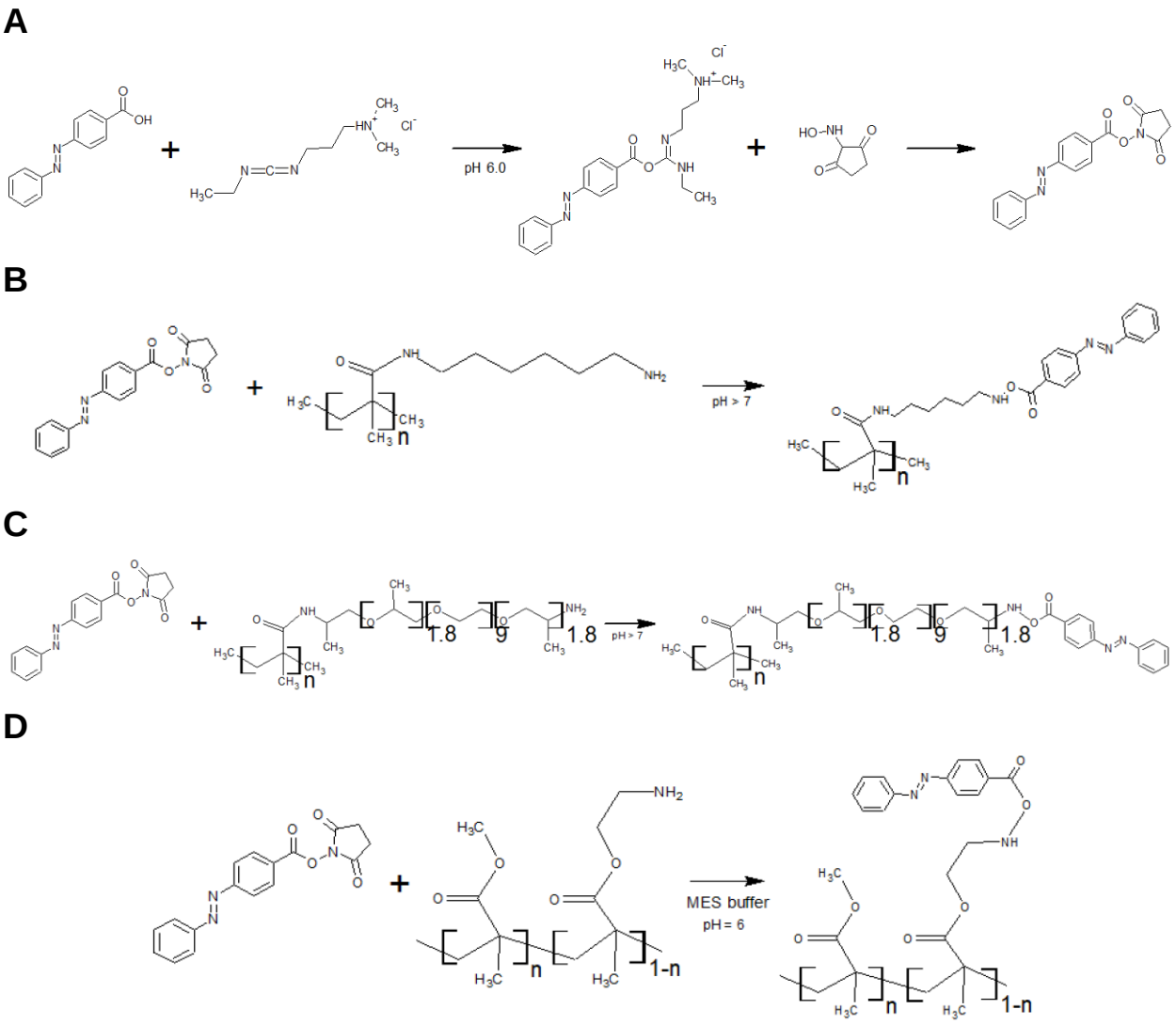

Figure 3.3: Reaction mechanisms for carbodiimide reaction of aminated PMMA surfaces and MMAcoAEM with 4-(phenylazo)benzoic acid. 4-(phenylazo)benzoic acid (AZO) is activated by EDC and stabilized by NHS (A). The NHS-AZO complex from (A) was then used to react with HMD (B) or PPG-PEG-PPG (C) aminated PMMA or MMAcoAEM (D).

MMAcoAEM was also bulk modified with azobenzene while dissolved in THF. A solution containing 30 mg of MMAcoAEM, 48.53 mg AZO, 82.29 mg EDC, and 49.41 mg NHS in 1 mL THF was reacted at room temperature in the dark for 24 h. After modification, the copolymer was precipitated out of solution by pouring the solution into 500 mL of water and extracting the polymer precipitate. A subsequent purification was performed on the polymer

through dissolution in THF and precipitation in water. Bulk modified MMAcoAEM was then rinsed with ethanol to remove unreacted 4-(phenylazo)benzoic acid and analyzed using NMR (dissolved in $CDCl_3$).

3.4.1. β-cyclodextrin complexation to azobenzene-modified surfaces

Modified samples were incubated in a solution of $1x10^{-3}$ M β-cyclodextrin (β-CD) in Millipore water to investigate the complexation of β-CD (in excess) with azobenzene at the surface. After incubation, samples were washed with 2 mL ethanol followed by 5 mL water and air-dried. Unmodified, amine, and azobenzene surfaces were analyzed using contact angles and photoisomerization studies before and after treatment with β-CD.

3.5. Changes in surface hydrophobicity measured using contact angles

Static sessile drop contact angles were measured to assess the hydrophobicity at the surface after each reaction. The contact angle is defined as the angle at the triple point between two liquids and a flat, solid surface at equilibrium. Contact angle measurements are commonly reported in literature and used to calculate surface properties including surface energy and curvature and can be used to determine the wettability of a surface. Polymer surfaces may change their characteristics over time due to re-orientation of free chains at the surface and roughness in a surface can introduce differences between the actual and apparent contact angles. Additionally, variations in temperature and the quality of the drop (liquid purity, equilibration time, size) may significantly impact contact angle development and stability.[119] Environmental conditions must be reported along with contact angle measurements and comparisons between experiments made while keeping these complex factors in mind.[119,120]

Static contact angles of 2 μL Millipore water droplets at 22 °C on unmodified, aminated, carboxylated, azobenzene-modified, and β-CD treated surfaces were measured using a DataPhysics Contact Angle System OCA 15EC digital goniometer and associated software. Sessile drops were dispensed from an electronically controlled syringe and formed on the sample by elevating a levelled stage. Static contact angles were analyzed on multiple areas of each disk and coated coverslip then averaged to minimize variations in drop quality. Measurements within sample sets were performed successively on the same day to minimize variations in temperature.

3.6. Surface elemental analysis via x-ray photoelectron spectroscopy

X-ray photoelectron spectroscopy (XPS) was used to analyze the chemical states and identify and quantify elements at the surface of PMMA before and after introducing amine groups and azobenzene. In this method, an aluminum (Al) x-ray source is used to excite the sample surface while under an ultra-high vacuum ($<10^{-9}$ Torr) to emit photoelectrons.[121] These electrons possess a kinetic energy dependent on the incident x-ray and the binding energy of its original atomic orbital. After the emitted electrons are collected by an electron energy analyzer, the binding energy and peak intensity are used to identify the chemical state and elements present at the surface. XPS gathers data from the top 10 nm of ultra-thin layers, provides up to 0.1% sensitivity to elemental composition, and may obtain a resolution from three to a few hundred micrometers: ideal for analyzing modifications to the thin surface layer of PMMA.[121] The detection limits for most elements are in the 1000 ppm range, however detection of lower ppm is possible if the elements of interest are concentrated at the surface or a long collection time is used (>5 h).

XPS was used to measure surface groups on coated coverslips but not PMMA disks due to technical difficulties with the disks degassing under high vacuum because of solvent retention. Prior to submitting samples for analysis, all samples were dried in a vacuum oven for 7 days to ensure they did not contain residual solvent or water. After sample submission, the polymer coated coverslips were mounted onto copper plates using adhesive tape due to the brittleness of the glass and to minimize charging effects on the sample. The samples were dried under high vacuum (10^{-9} Torr) overnight then transferred to the analysis chamber (10^{-10} Torr). Spectra were collected on a Kratos Nova AXIS spectrometer using AlK_{α} radiation at 1486.69 eV (150 W, 15 kV), charge neutralizer, and a delay-line detector consisting of three multi-channel plates. High resolution spectra were recorded with a pass energy of 20 eV and dwell time of 300 s over a 300 × 700 μm^2 area (lens mode: FOV 1). The spectra were measured using *Vision 2* software (Kratos Analytical) and processed using *CasaXPS* software (Neal Farley) with binding energies referred to the C 1s peak at 285 eV. Data was corrected for energy shifts due to charging of the sample and the spectra were corrected for background using the Shirley algorithm. The assignments of the chemical groups are based on the binding energies reported in literature.[122–125]

3.7. Ultraviolet-visible spectroscopy to investigate azobenzene photoisomerization

Ultraviolet-visible (UV-VIS) spectroscopy was used to verify the presence of azobenzene on modified surfaces and to monitor the photoisomerization of azobenzene between the *trans*- and *cis*- conformations. The wavelengths of maximum absorption for the *trans*- and *cis*-forms of 4-(phenylazo)benzoic acid in ethanol were measured to be 326 nm and 440 nm respectively. After irradiation at this wavelength, some molecules absorb energy to convert to the

other form. This transition is measurable through the shift in peak area under a wavelength vs. absorbance plot, as shown in Figure 3.4.

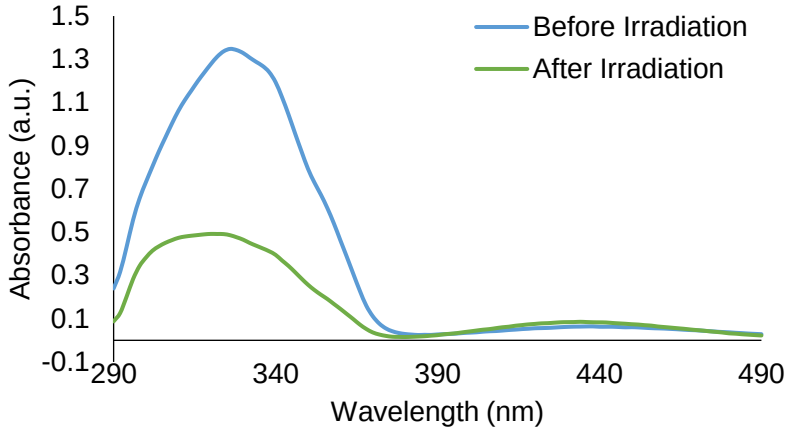

Figure 3.4: Absorbance curve for $1x10^{-4}$ M azobenzene in ethanol before (blue) and after (green) 2 h irradiation with 365 nm light. Before irradiation at 365 nm, the majority of azobenzene is found in the *trans*- form, however a significant portion of these molecules isomerize after irradiation to the *cis*- form, resulting in a smaller peak at 326 nm.

The photoisomerization of azobenzene-modified coated coverslips was investigated by placing the coatings in a well plate covered by 1 mL Millipore water and irradiating with a UVP UVL-21 compact UV lamp (4 W, 115 V ~ 60 Hz, 0.16 A) at 365 nm for 0 – 2 h at 5 cm above the sample surface. The power at the sample surface is expected to be inversely proportional to the distance from the UV lamp and reduced after travelling through the water, but was not measured directly. At 30 min intervals, the absorbance was measured using a Perkin Elmer Enspire Multimode Plate Reader in the range of 270 – 500 nm. Unmodified and amine-functionalized coatings were used as negative controls.

UV-VIS spectroscopy was also used to monitor the attachment of β-CD to azobenzene-modified coverslips. PPG-PEG-PPG coverslips before and after azobenzene modification were tested as they had the best chain mobility to minimize steric hindrances to the photoisomerization.

Samples with β-CD bound to azobenzene are expected to have a lower absorbance than samples without β-CD. Each coverslip was incubated in excess β-CD (1 mL of $1x10^{-3}$ M) in Millipore water for 1 h then rinsed twice with 5 mL Millipore water. The coverslips were placed in a well plate covered in 1 mL water to dissolve any β-CD detaching from surfaces. The surfaces were irradiated for 1 h at 365 nm using a UVP UVL-21 compact UV lamp (4 W, 115 V ~ 60 Hz, 0.16 A) 5 cm above the sample surface. At 30 min intervals, the absorbance of the coverslips in solution was measured using a Perkin Elmer Enspire Multimode Plate Reader from 270 – 500 nm and the wells replenished with 1 mL of fresh Millipore water. Unmodified PMMA and PPG-PEG-PPG-modified PMMA coatings were used as negative controls.

3.8. HL-60 cell culture on PMMA and amine- and carboxyl-functionalized PMMA

The viability and adhesion of neutrophil-like cells on functionalized PMMA was studied by incubating HL-60 cells with aminated and carboxylated PMMA disks. HL-60 viability experiments were conducted on smoothed functionalized PMMA as rough surfaces are known to decrease the cell adhesion and proliferation of lens epithelial cells and induce neutrophil cell death.[14,126]

HL-60 cells were cultured in Iscove's Modified Dulbecco's Medium (IMDM) with 20% fetal bovine serum (FBS) and 1% penicillin/streptomycin solution, incubated at 37 °C in 5% carbon dioxide and 95% air, and passaged to maintain 100,000 – 1,000,000 cells/mL. HL-60 cells were activated with 50 nM phorbol-12-myristate 13-acetate (PMA) to promote differentiation into a neutrophil/macrophage-like phenotype[51,52] which also promotes their adhesion. In addition to azobenzene modifications, preliminary studies were performed on HL-60 cells cultured on

aminated and carboxylated PMMA disks. The study was conducted to investigate how surface functional groups affect neutrophil-like cell viability and adhesion on PMMA. Human promyelocytic leukemia (HL-60) cells were used for cell studies as they continuously proliferate and may be differentiated to possess qualities of granulocytes, monocytes, and macrophages with detailed HL-60 differentiation protocols discussed in literature.[47,50,51]

HL-60s were incubated with PMMA disks of different chemistries and then analyzed using the alamarBlue® assay or deoxyribonucleic acid (DNA) stains. PMMA disks were sterilized with two 15 minute washes in 70 % ethanol, air dried, and incubated overnight in 0.5 mL of medium. The medium was removed from disks and 0.5 mL of a 600,000 cell/mL solution added. HL-60 cells were incubated with the disks for 48 hours with 50 nM PMA or without PMA as controls.

3.8.1. Surface topography investigated using atomic force microscopy

Prior to cell culture, the topology of PMMA smoothed and unsmoothed disks were measured using atomic force microscopy (AFM) as roughness has been linked to cell proliferation and migration in literature.[20,127] AFM is a scanning probe method which measures local properties of a surface using a cantilever tipped with a sharp probe. As the probe moves towards the surface, attractive then repulsive forces between the probe and the surface cause deflections in the cantilever. These deflections are measured by directing a laser onto the back of the cantilever and using a position-sensitive photo diode to track changes in the reflected beam. AFM can operate in three different modes: contact mode, tapping mode, and non-contact mode. Contact mode

maintains a constant height or force as it scans across a surface while non-contact and tapping modes oscillate above the surface with a constant amplitude.

AFM was used to measure the roughness of the smoothed PMMA disks as it can be used to develop images with angstrom-level resolution and three-dimensional topography while requiring minimal sample preparation. A Veeco Multimode Atomic Force Microscope operating in tapping mode was used to analyze PMMA since this mode provides higher lateral resolution and faster scan time than non-contact mode and is less-damaging and less likely to distort topographical images than contact mode. A topographical heat map was developed for three 100 μm^2 areas on a smoothed and unsmoothed PMMA disk with root mean square roughness (Rq) and average roughness (Ra) reported.

3.8.2. HL-60 viability was measured using an alamarBlue® assay

An alamarBlue® assay was performed to assess cell viability of HL-60 cells incubated with and without PMMA and functionalized PMMA. The alamarBlue® reagent contains a non-toxic, cell-permeable, and barely fluorescent compound named resazurin. Active cells maintain a reducing environment in the cytosol, and upon entering cells resazurin is reduced to the highly fluorescent compound resorufin. Living cells continually convert resazurin to resorufin causing the surrounding media to change colour and overall fluorescence to increase. The alamarBlue® assay compares the absorbance of resazurin at 600 nm and resorufin at 570 nm to measure cell activity. After 48 hours, the medium was aspirated and the disks/wells gently rinsed with 0.5 mL of phosphate buffered saline. Each disk/well (with adhered HL-60 cells or controls minimal adhered cells) were next incubated for 4 h in 0.05 mL of alamarBlue® reagent and 0.45 mL media.

The absorbance of the resulting solutions was read at 570 nm and 600 nm using 200 μL samples in duplicate with a Perkin Elmer Enspire Multimode Plate Reader. Results are reported as absorbance ratios 570 nm/600 nm with the absorbance from blank wells containing only media subtracted as background.

3.8.3. DNA staining to determine the live/dead cell ratios on PMMA surfaces

In addition to investigating the activity of cells seeded on PMMA disks, the DNA content inside and outside of cells was assessed using DNA staining. This information is important to understand the dynamics of HL-60 cells while attached to PMMA and how functional groups at the surface may influence cell behaviour. Intracellular staining of DNA indicates live cells while extracellular staining indicates dead cells or extracellular traps.

Unfunctionalized, COOH- and NH_2-PMMA disks were each seeded with HL-60 cells by adding 0.5 mL of a solution containing 600,000 cells/mL to each sample in a well plate. This solution contained modified medium made of 450 mL of IMDM, 5 mL of penicillin/streptomycin solution, and 90 mL of heat-inactivated FBS. Three samples of each surface chemistry were incubated with 0.5 mL of 50 nM PMA to promote cell adhesion, while three samples of each surface chemistry were stained without adding PMA as controls. After incubating for 48 h, one drop of NucBlue® Live Cell ReadyProbes Reagent was added to each well to stain intracellular DNA. Disks were incubated at 37^{o}C and 5% CO_2 / 95% air for 20 min, rinsed twice using 0.5 mL sterile PBS, then incubated in 10% formalin for 10 min at room temperature to fix the cells. After fixation with formalin, disks were again rinsed twice with 0.5 mL phosphate buffered saline (PBS), and then incubated with 0.5 mL of $1.7x10^{-3}$ nM SYTOX® green solution to stain extracellular

DNA. The stained samples were rinsed twice with 0.5 mL PBS. Disks were preserved by adding one drop of anti-fade to the surface, covering the surface with a round glass coverslip, drying overnight, and sealing the edges with nail polish. An EVOS FL Cell Imagining System was used to produce five overlay images at 20 times magnification for each disk (approximately 420 μm x 560 μm area), with each overlay having a transference image, and excitation/emission maxima images at 358 nm/461 nm (blue light) and 488 nm/510 nm (green light). ImageJ software (National Institutes of Health, Bethesda, Maryland, USA) was used to perform area counts of blue and green stains for each surface, with stains less than 80 μm^2 discarded as anomalies. Blue stains represent live cells while green stain represents cells either dead or undergoing NETosis. The live cells stained and the ratio of NETosis to the total DNA stained are reported.

3.9. Statistics

Data sets containing multiple trials with replicate samples are reported with standard error measurements while all other samples are reported with standard deviation. Two-tailed Student's t-tests were used to examine significant differences between samples using a 95% confidence interval and assuming unequal variance and a normal distribution.

Chapter 4. Results

4.1. Surface functionalization of PMMA disks with amine and carboxylic acid groups

The first set of experiments focused on the functionalization of poly(methyl methacrylate) (PMMA) disks. PMMA disks were smoothed and functionalized with either amine or carboxyl groups using wet chemical methods. After optimizing the graft densities, functionalized surfaces were used to culture HL-60 cells with phorbol 12-myristate 13-acetate (PMA) to induce differentiation and cell adhesion.

4.1.1. Surface topography of rough and smoothed PMMA disks

Atomic force microscopy (AFM) was used to assess the surface roughness of PMMA disks before and after smoothing with chloroform. Three separate areas on one smoothed and one rough disk were analysed, with roughness and representative images given in Table 4.1 and Figure 4.1. The range of height of the rough disk was three to six times that of the smoothed disk across the three sample areas. The average root mean square (Rq) and mean (Ra) roughness values were both statistically different between the rough and smooth disks ($p = 0.0074$ for rough, $p = 0.0054$ for smooth). Rough disks were also consistently more hydrophobic than smoothed disks with contact angles of 80 ± 2 ° and 76 ± 1 ° respectively, although not significantly different ($p = 0.075$). X-ray photoelectron spectroscopy (XPS) results confirmed that smooth surfaces had a slightly higher amount of polar, hydrophilic groups at the surface (Appendix A.1). An increase in hydrophobicity with roughness is hypothesized to be due to the smoothing procedure decreasing the amount of entrapped air at the surface of the polymer, thus increasing hydrophilicity.

A.2

Table 4.1: Average root mean square (Rq) and mean (Ra) roughness of rough and smoothed PMMA disks reported with standard deviation. (n = 3).

	Rq (nm)	Ra (nm)
Rough Disk	14.3 ± 2.2	9.5 ± 1.2
Smooth Disk	1.8 ± 0.3	1.3 ± 0.2

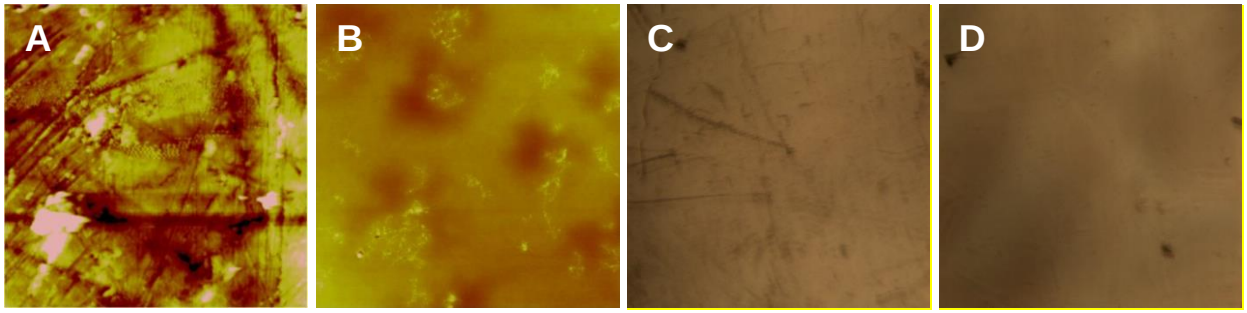

Figure 4.1: Heat-map AFM images of a 10 μm x 10 μm area of rough (A) and smoothed (B) PMMA indicate surface topology, with darker colours being indents in the surface and lighter colours being protrusions. XPS images of rough (C) and smooth (D) PMMA show that the rough disk has an abundance of both shallow and deep imperfections in the surface while smoothed disks are more uniform.

4.1.2. Surface functionalization of PMMA disks

4.1.2.1. Aminolysis functionalization of PMMA disks

Amine functionalization was performed based on the method developed by Fixe *et al*.[1] First the pH and length of reaction were varied in an attempt to maximize the hexamethylenediamine (HMD) graft density at the surface. Using a ninhydrin assay to quantify the amine functionalization, it was determined that increasing the pH and reaction time increased the amine graft density, shown in Figure 4.2. The results are reported as the difference between unfunctionalized PMMA and amine-functionalized PMMA. The amine density was significantly higher on functionalized surfaces than on unfunctionalized controls for PMMA reacted at pH 11.5 for 48 h ($p = 0.04$) and pH 12.5 for 2 h ($p = 0.03$), but not for PMMA reacted at pH 11.5 for 2 h ($p = 0.16$) or pH 12.5 for 48 h ($p = 0.06$).

Interestingly, the reaction conditions from Fixe *et al.* (pH 11.5 for 2 h) produced significantly less amine functionality than the pH 11.5 for 48 h ($p = 0.05$), pH 12.5 for 2 h ($p = 0.04$), and pH 12.5 for 48 h ($p = 0.05$) conditions. The pH 11.5 for 48h, pH 12.5 for 2h, and pH 12.5 for 48h results were not significantly different from each other ($p = 0.39$ for pH 11.5 for 48 h/ pH 12.5 for 2 h, $p = 0.39$ for pH 11.5 for 48 h/ pH 12.5 for 48 h, and $p = 0.42$ for pH 12.5 for 2 h/pH 12.5 for 48 h). Further experiments using PMMA disks and PMMA-coated coverslips (later sections) were performed using PMMA aminated at pH 12.5 for 2 h because the increased pH increased the number of amine groups, with insignificant differences between 2 h and 48 h.

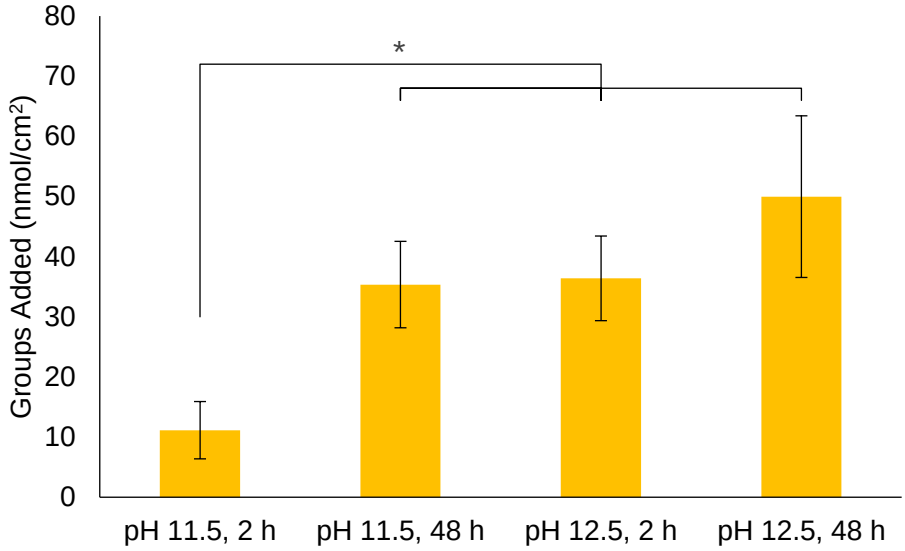

Figure 4.2: Ninhydrin results with standard error (SE) bars for aminolysis reaction of PMMA with HMD while varying pH and reaction time. ($n = 3$, $*p < 0.01$).

PMMA disks were also modified with a longer diamine spacer O,O'-bis(2-aminopropyl) propylene glycol-block-polyethylene glycol-block-polypropylene glycol (PPG-PEG-PPG) using a pH 12.5 for 2 h with ninhydrin results below. Both HMD and PPG-PEG-PPG surfaces had a significantly higher amine content than unmodified controls ($p = 0.04$ for HMD, $p = 0.04$ for

PPG-PEG-PPG). There was no significant different between the HMD and PPG-PEG-PPG graft densities ($p = 0.09$).

Table 4.2: Ninhydrin quantification for the amine modification of PMMA disks with either the short (HMD) or long (PPG-PEG-PPG) diamine spacer reported with standard error. (n = 3).

PMMA Disk	Amine Groups (nmol/cm^2)
+ HMD	36.4 ± 7.0
+ PPG-PEG-PPG	19.5 ± 3.0

4.1.2.2. Hydrolysis optimization and quantification

A separate functionalization converting the ester groups to carboxyl groups on PMMA was investigated using two different solutions of methanol and sodium hydroxide (n = 3). The first reaction tested a 1:1 ratio of 1 N NaOH and methanol for 1 h, however modified samples did not have significantly different functional groups than unmodified controls. Next, the reaction time and concentration of NaOH were increased to drive the hydrolysis reaction. The carboxyl content of 1 N NaOH for 6 h was 211.8 ± 63.5 nmol/cm^2, in 6 N NaOH for 2 h was 174.8 ± 39.4 nmol/cm^2, and in 6 N NaOH for 6 h was 208.7 ± 51.8 nmol/cm^2. There were no significant differences when reacting with 1 N NaOH for 6 h or using 6 N NaOH for either 2 h or 6 h ($p = 0.70$ for 1 N for 6 h and 6 N for 2 h, $p = 0.98$ for 1 N for 2 h and 6 N for 6 h, $p = 0.69$ for 6N 2 h and 6 N 6 h), suggesting the reaction completes before 2 h. The 6 N for 6 h carboxyl-functionalized surfaces were used for HL-60 cell culture studies, discussed in detail in Section 4.5. Additional characterization should be used to verify the carboxyl concentration, since it was assumed that the surface was perfectly smooth for quantification however the AFM results indicated that smoothed PMMA still contained some roughness.

4.1.2.3. Azobenzene modification

The aminated PMMA disks were reacted with azobenzene in a pH 6.0 2-(N-morpholino)ethanesulfonic acid (MES) buffer for 24 h in the dark. For HMD-modified PMMA disks, a significant 56% reduction in amine groups was measured ($p = 0.04$). There was also a reduction in the number of amine groups on PPG-PEG-PPG surfaces, however the change was not significant ($p = 0.50$).

Table 4.3: Ninhydrin assay results for azobenzene modification of PMMA disks with standard error. Graft densities were compared to amine-functionalized PMMA controls (short spacer HMD, long spacer PPG-PEG-PPG) to calculate the azobenzene (AZO) graft density and reaction yield as the percentage of amine groups converted to azobenzene groups. ($n = 3$).

PMMA Disk	Amine Groups ($nmol/cm^2$)	AZO Groups ($nmol/cm^2$)	Yield of AZO Reaction
+ HMD + AZO	36.4 ± 7.0	20.5 ± 0.4	56 %
+ PPG-PEG-PPG + AZO	19.5 ± 3.0	2.20 ± 0.2	11 %

4.1.2.4. Functionalizing PMMA increased hydrophobicity of the surface

Static contact angles were measured to determine the effect of functionalization on surface hydrophobicity, with a summary in Table A.2 in Appendix A.2. A variety of reaction conditions from the amine and carboxyl modification were tested. The contact angles of most functionalizations were significantly different than smooth PMMA, including rough PMMA ($p = 0.05$), HMD (b) ($p = 0.04$), HMD (d) ($p = 0.009$), carboxyl (a) ($p = 0.01$), and carboxyl (b) ($p = 0.04$), but excluding HMD (a) ($p = 0.93$), HMD (c) ($p = 0.25$), and the PPG-PEG-PPG ($p = 0.32$) modifications.

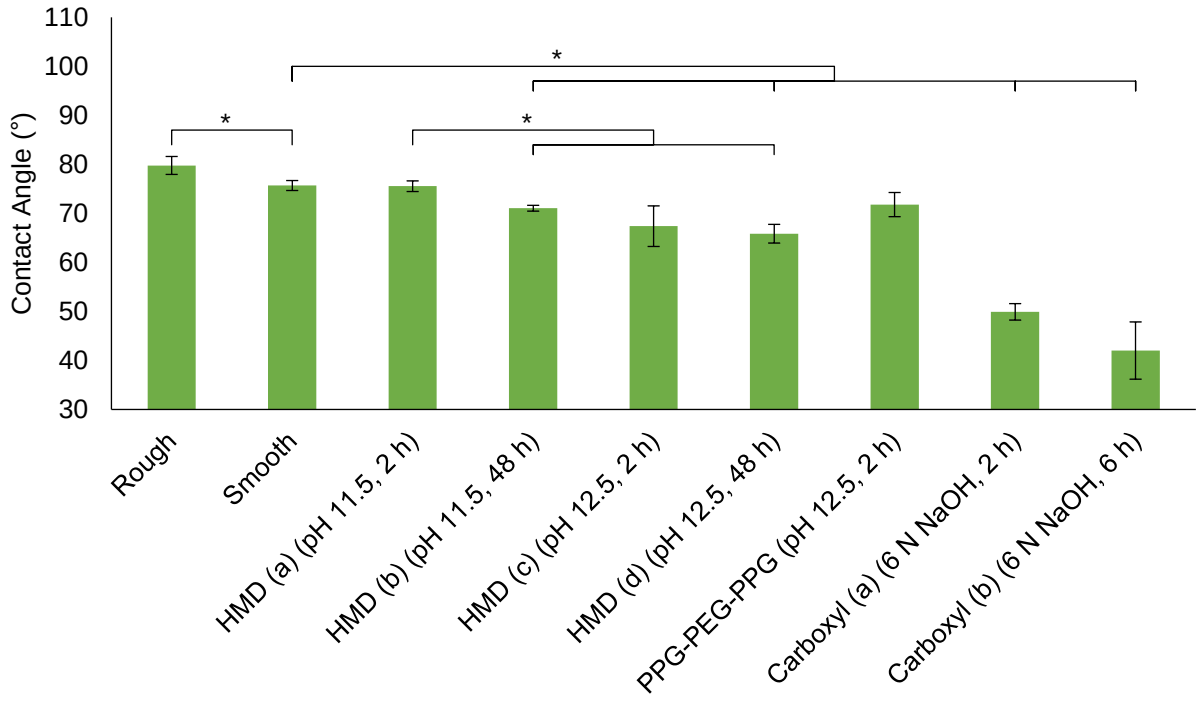

Figure 4.3: Static water contact angles for unmodified and amine (short spacer HMD, long spacer PPG-PEG-PPG) and carboxyl functionalized PMMA disks with standard error bars. (n = 3, *$p < 0.05$). For a table of values please refer to Appendix A.2.

The contact angle of HMD (a) was significantly higher than the contact angles of HMD (b) ($p = 0.02$) and HMD (d) ($p = 0.01$). The lack of significant difference between the HMD modified (b), (c) and (d) samples further suggests the amine modification goes to completion before a reaction time of 2 h. These contact angles support the ninhydrin assay results, where increasing pH and reaction time increase hydrophilicity. Together these results were used to determine 2 h as the reaction time for further amine modifications. There was no significant difference between the carboxyl reaction conditions (a) and (b) ($p = 0.21$). Figure 4.4 summarizes contact angles after azobenzene modifications and after incubation with β-cyclodextrin (β-CD) (values in Table A.3 in Appendix A.2). After modification with azobenzene, there was no significant change in contact angle for HMD ($p = 0.39$) or PPG-PEG-PPG disks ($p = 0.88$). There was a significant increase in water contact angle after incubation in β-CD for HMD + AZO

(p = 0.04), but not for smooth PMMA (p = 0.32), HMD (p = 0.16), PPG-PEG-PPG (p = 0.26), or PPG-PEG-PPG + AZO (p = 0.53) surfaces. It is hypothesized that β-CD may be inducing a rearrangement of surface chains, resulting in an increase in hydrophobicity after incubation as opposed to the expected increase in hydrophilicity associated with the exterior of β-CD.

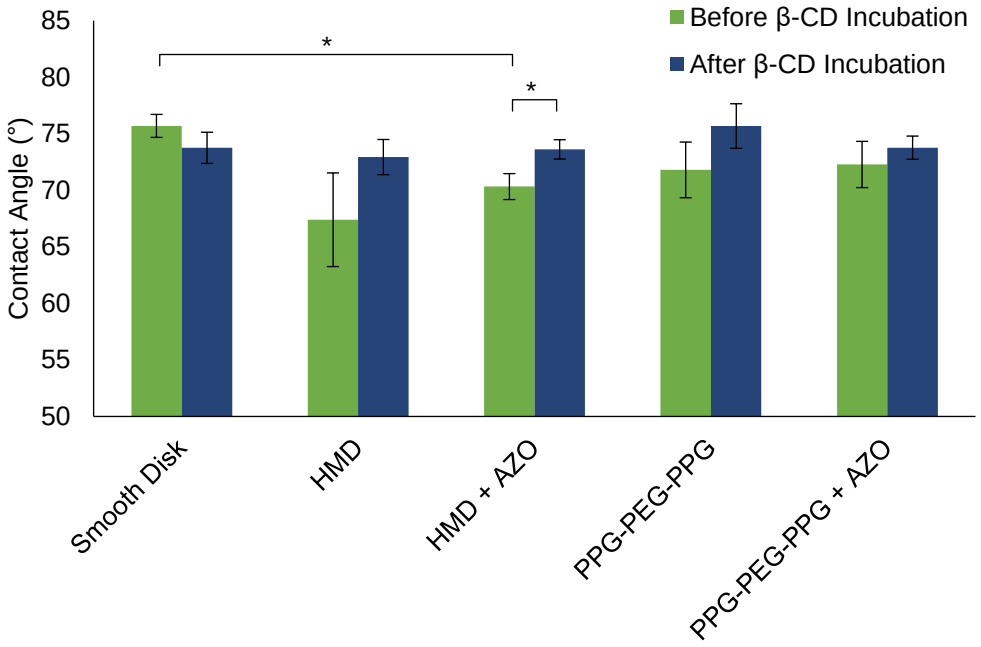

Figure 4.4: Static water contact angles for PMMA disks before and after incubation in a $1x10^{-3}$ M β-cyclodextrin (β-CD) in water with standard error bars. Unmodified PMMA smooth disks and amine modified disks (short spacer HMD, long spacer PPG-PEG-PPG) were used as controls for azobenzene-modified (AZO) disks. (n = 3, *p < 0.05). For values please refer to Appendix A.2.

4.2. Surface modification of PMMA-coated coverslips

Azobenzene modifications were performed on surfaces coated with a thin layer of PMMA to obtain materials better suited to XPS and UV-VIS spectroscopy analysis. The average thickness of PMMA-coated coverslips was measured to be 0.11 ± 0.01 mm using a digital caliper.

4.2.1. Amine graft density of PMMA-coated coverslips

PMMA-coated coverslips were functionalized with amine for 2 h in pH 12.5 buffer on PMMA-coated coverslips, with ninhydrin results summarized in Table 4.4. The amine density was significantly higher on HMD ($p = 0.0003$) and PPG-PEG-PPG ($p = 0.01$) compared to unfunctionalized PMMA controls. There was no significant difference between the graft density on HMD and PPG-PEG-PPG surfaces ($p = 0.81$).

Table 4.4: Ninhydrin assay results for amine modification of PMMA-coated coverslips with short spacer (HMD) or long spacer (PPG-PEG-PPG) with standard error. (n = 3).

PMMA Coated Coverslip	Amine Groups ($nmol/cm^2$)
+ HMD	21.1 ± 0.9
+ PPG-PEG-PPG	20.3 ± 2.9

4.2.2. Azobenzene modification of PMMA-coated coverslips

Amine functionalized PMMA-coated coverslips were then modified with azobenzene groups. There was a significant reduction in the amine groups on PPG-PEG-PPG surface after azobenzene modification ($p = 0.04$) but the change in amine groups on the HMD surface was not significant ($p = 0.06$).

Table 4.5: Ninhydrin results for azobenzene (AZO) modification of PMMA-coated coverslips with standard error. Graft densities were compared to amine-modified controls (short spacer HMD, long spacer PPG-PEG-PPG) to calculate the azobenzene graft density and reaction yield as the percentage of amine groups converted to azobenzene groups. (n = 3).

PMMA Coated Coverslip	Amine Groups ($nmol/cm^2$)	AZO Groups ($nmol/cm^2$)	Yield of AZO Reaction
+ HMD + AZO	21.1 ± 0.9	3.4 ± 0.2	16 %
+ PPG-PEG-PPG + AZO	20.3 ± 2.9	11.2 ± 2.6	55 %

4.2.3. Surface hydrophobicity changes with azobenzene- and β-cyclodextrin modification

Contact angles were recorded for PMMA-coated coverslips before and after each modification stage and after incubation in a solution of β-CD in water, summarized in Figure 4.5 (values in Table A.4 in Appendix A.2). Similar to results obtained for PMMA disks, the amine modification caused the surfaces to become more hydrophilic. Functionalizing PMMA significantly lowered the contact angle from 75 ± 2 ° to 69 ± 2 ° for PPG-PEG-PPG ($p = 0.02$), but not for HMD ($p = 0.07$). HMD and PPG-PEG-PPG contact angles were also significantly different ($p = 0.03$).

Azobenzene modification did not significantly impact the static contact angle of HMD ($p = 0.71$) or PPG-PEG-PPG ($p = 0.07$) coverslips. After incubation in β-CD, the contact angles significantly decreased from 75 ± 2 ° to 67 ± 2 ° for PMMA coverslips ($p = 0.0005$) and from 72 ± 1 ° to 65 ± 4 ° for PPG-PEG-PPG+AZO coverslips ($p = 0.03$) and significantly increased from 69 ± 2 ° to 74 ± 1 ° for PPG-PEG-PPG coverslips ($p = 0.009$). Non-specific adsorption of β-CD could be responsible for the decrease in unmodified PMMA contact angle, however the increase in contact angle for PPG-PEG-PPG may indicate that surface rearrangement is occurring.

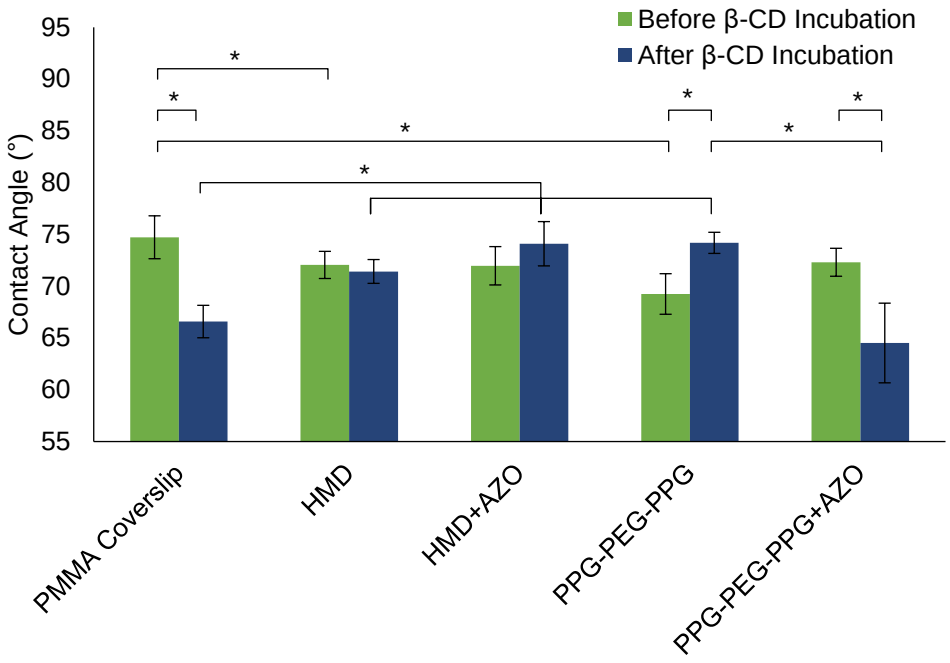

Figure 4.5: Static water contact angles for unmodified, amine-modified (short spacer HMD, long spacer PPG-PEG-PPG), and azobenzene-modified (AZO) PMMA-coated coverslips before and after incubation with $1x10^{-3}$ M β-cyclodextrin (β-CD) in water with standard error bars. (n = 3).

4.2.4. Elemental analysis of the surface via x-ray photoelectron spectroscopy

XPS spectra of amine-modified PMMA-coated coverslips support the ninhydrin results for the amine modification. Attachment of the diamine tether to the surface should result in an increase in N 1s and C 1s C-C peaks and a decrease in the ester O 1s C-O peak from PMMA. These changes were present for both HMD and PPG-PEG-PPG modified surfaces, in addition to a decrease in C 1s C(O)C and increases in O 1s and C 1s C=O peaks, further suggesting the PMMA ester functionality decreased after modification.

Table 4.6: XPS results for PMMA-coated coverslips reported as Atomic Concentration (At %). Green values increased from PMMA to PPG-PEG-PPG modified or from PMMA to HMD modified surfaces while orange values decreased. (n = 1).

	PMMA		PMMA + HMD		PMMA + PPG-PEG-PPG	
	Position	At %	Position	At %	Position	At %
Na 1s			1071.44	0.39		
O 1s, C-O	533.85	12.35	533.96	10.81	533.89	11.01
O 1s, C=O	532.28	12.44	532.37	13.37	532.41	12.97
N 1s, NHC=O				0.26	401.64	0.13
N 1s	400.3	0.27	400.19	0.58	400.21	0.3
C 1s, C(O)O	289.04	14.11	289.14	12.32	289.13	11.38
C 1s, C=O			286.73	10.95	287.19	5.44
C 1s, C-O	286.84	13.13	287.37	3.86	286.63	11.27
C 1s, C-C	285.74	17.79	285.7	19.18	285.7	17.83
C 1s, CH_x-C	285	29.92	285	26.77	285	28.11
Cl 2p1/2			199.62	0.09	199.59	0.03
Cl 2p3/2			197.89	0.18	197.73	0.06
Si 2p, SiO			102.3	1.24	102.27	1.46

Chlorine and silicon impurities were only detected in modified samples and not in the unmodified PMMA-coated coverslip. Interestingly, the O 1s C-O peak decreased for the PPG-PEG-PPG sample and there was only a slight increase in the C 1s C-C peak although PPG-PEG-PPG contains more C-O and C-C bonds than a native PMMA methyl ester group. Additionally, for both modifications the methyl CHx-C peak decreased. To verify the atomic concentrations measured in XPS, replicate samples should be analyzed and multiple areas on each modified surface should be analyzed to ensure a homogeneous distribution of functional groups.

4.3. Copolymer MMAcoAEM

To increase the amount of azobenzene grafted to surfaces, a copolymer of methyl methacrylate (MMA) and 2-aminoethyl methacrylate (AEM) was synthesized with a higher prevalence of amine groups than previous amine modified surfaces. The copolymer was soluble

in chloroform and THF, and similarly to PMMA was clear and colourless when solution-coated onto surfaces. The amine content of the copolymer was estimated with a ninhydrin assay and the structure investigated using proton (^{1}H) NMR, then the copolymer was modified with azobenzene in the bulk and on coated coverslips.

4.3.1. MMAcoAEM contained more amine groups than functionalized-PMMA

The ninhydrin assay was used to estimate the amount of amine groups in the MMAcoAEM in bulk and on the surface of coverslips. The bulk concentration of amine was also used to estimate the percentage of the AEM monomer in MMAcoAEM. Despite attempting to synthesize 40 mol% AEM, comparing the bulk ninhydrin measurement to the theoretical amine content of the copolymer, the true copolymer amine content is estimated at 0.7 mol% AEM. MMAcoAEM was not soluble in the ninhydrin reagent solution, therefore it is likely that some amine functionality was not measured by the assay as ninhydrin is unable to penetrate the polymer.

MMAcoAEM-coated coverslips contained twice as many amine groups as amine-modified PMMA-coated coverslips at 44.0 ± 2.2 nmol/cm^2 compared to 21.1 ± 0.9 nmol/cm^2. The MMAcoAEM bulk material contained six times as many amine groups as amine-modified PMMA-coated coverslips, with $3.7 \times 10^{-11} \pm 5.0 \times 10^{-12}$ mol AEM/g MMAcoAEM (equivalent to 129.6 ± 17.8 nmol/cm^2 if coated) compared to 21.1 ± 0.9 nmol/cm^2. The number of amine groups on MMAcoAEM-coated coverslips was significantly below the bulk concentration ($p = 0.002$), possibly due to association of the positively charged amine groups with the negatively charged glass coverslip. However, a ninhydrin assay comparing peeled and non-peeled coverslips revealed no significant difference in amine concentration ($p = 0.85$). There remains a large area for

improvement of the amine content of the copolymer. Other methods of polymerization which improve the homogeneous distribution of amine groups in the copolymer should be explored, such as atom transfer radical polymerization (ATRP).[128–130]

4.3.2. Structure analysed using nuclear magnetic resonance spectroscopy

The proton nuclear magnetic resonance (NMR) spectrum of MMAcoAEM complemented the ninhydrin assay results but was also inconclusive. Based on ^{1}H NMR studies of the AEM monomer and poly AEM, the peaks from H on the ethylamine side group are expected to appear around δ = 2.9 ppm and δ = 4.1 ppm in D_2O.[67,128,131,132] The MMAcoAEM copolymer demonstrates isotactic structure of PMMA in the δ = 1.0 ppm to δ = 2.0 ppm region and there are two distinctly new peaks at δ = 2.3 ppm and δ = 5.0 ppm, which may correspond to the shifted peaks of the H on the ethylamine group of AEM (Figure 4.6 C and D). Based on the ninhydrin results, only 0.7 mol% of the copolymer contains amine groups, making detection of these groups in proton NMR difficult. The suspected amine peaks are also similar in height to impurity peaks thought to result from residual benzoyl peroxide (BPO) at δ = 7.6 ppm and δ = 8.1 ppm.[133] Further NMR studies are required to verify the structure of MMAcoAEM and the amine content of the polymer will remain estimated using the ninhydrin assay for these studies.

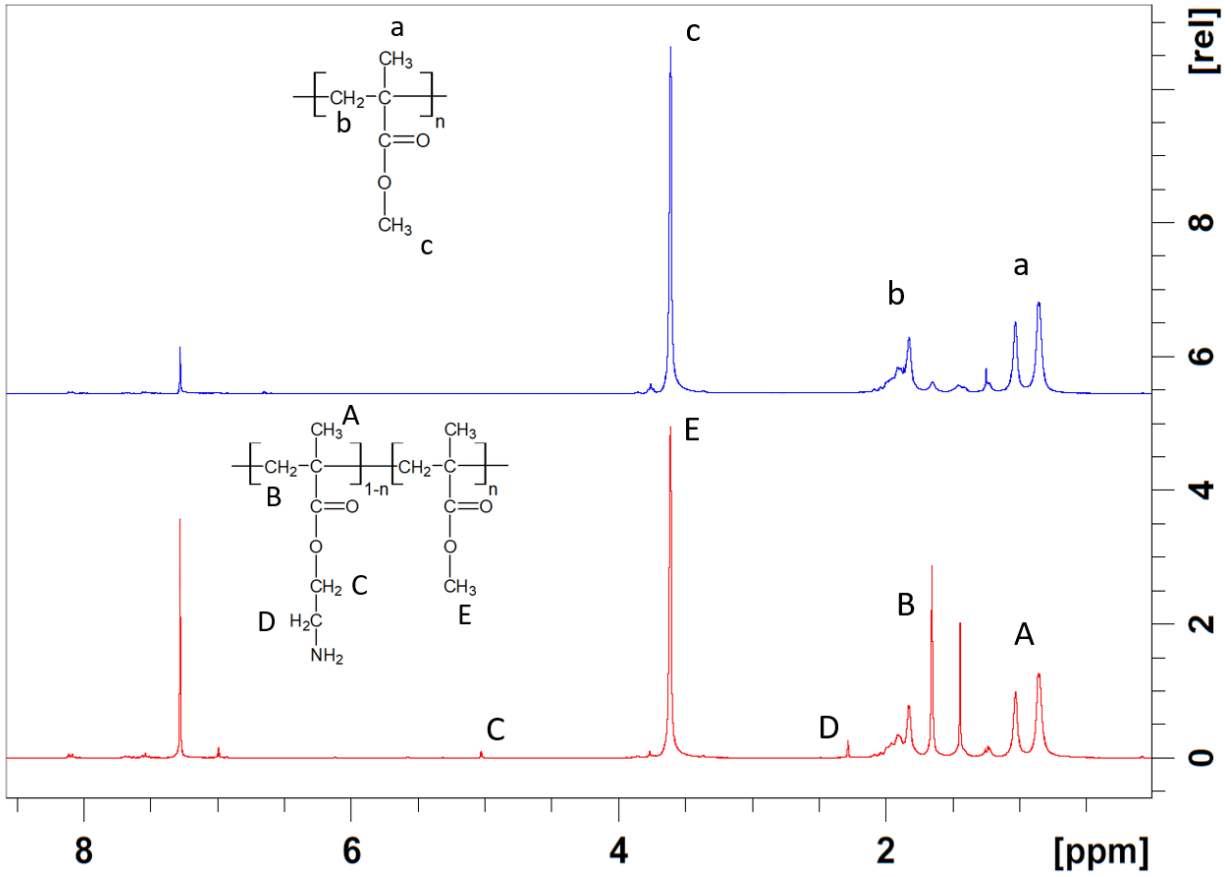

Figure 4.6: Proton NMR spectra for 20 mg of dissolved PMMA (blue) or MMAcoAEM (red) in deuterated chloroform ($CDCl_3$, δ = 7.26 ppm).

4.3.3. Azobenzene modification of MMAcoAEM

The MMAcoAEM copolymer was modified with azobenzene groups and the degree of modification was estimated by measuring the number of amine groups remaining at the surface. There was a 41 % reduction in amine groups on MMAcoAEM-coated coverslips and 19 % reduction in bulk amine groups after azobenzene modification. The MMAcoAEM-coated coverslip amine density decreased from 44.0 ± 2.2 nmol/cm^2 to 25.9 ± 8.9 nmol/cm^2, however the change was not significant (p = 0.11). Similarly, the amine content of the bulk MMAcoAEM decreased from 3.7x10^{-11} ± 5.0x10^{-12} mol AEM/g MMAcoAEM to 3.0x10^{-11} ± 2.1x10^{-12} mol AEM/g MMAcoAEM (equivalent to 104.8 ± 7.5 nmol/cm^2 if coated), but not significantly (p =

0.25). The bulk reaction of MMAcoAEM in THF had a lower yield of azobenzene modification despite having the largest number of amine groups available for reaction. Early renditions of the modification mechanism investigated ethanol as a solvent for the carbodiimide reaction, similarly leading to minimal changes in amine graft density. The availability of protons and the charge of functional groups in solution strongly contribute to the efficiency of both EDC/NHS coupling and the preconcentration of amine groups at the reaction site.[58,134] As such, the MES pH 6.0 buffer was identified to be the most effective reaction medium. Comparing these results to PMMA-HMD and PMMA-PPG-PEG-PPG modified with azobenzene, there were no apparent trends between the length of amine-terminated spacer (or AEM group) and the resulting graft density of azobenzene.

Table 4.7: Ninhydrin assay results for azobenzene modification of MMAcoAEM bulk and MMAcoAEM-coated coverslips with standard error. Graft densities were compared to unmodified MMAcoAEM controls to calculate the azobenzene (AZO) graft density and reaction yield as the percentage of amine groups converted to azobenzene groups. (n = 3).

Copolymer	Reaction Media	Amine Groups ($nmol/cm^2$)	AZO Groups ($nmol/cm^2$)	Yield of AZO Reaction
Coverslip + AZO	MES buffer pH 6	44.0 ± 2.2	18.1 ± 8.9	41 %
Bulk + AZO	THF	129.6 ± 17.8	24.8 ± 4.4	19 %

4.3.4. Azobenzene-modification of MMAcoAEM increased surface hydrophobicity

Contact angles were measured for the MMAcoAEM-coated coverslip before and after azobenzene modification and incubation in β-CD in water (values in Table A.5 in Appendix A.2). The contact angle of MMAcoAEM was significantly more hydrophilic than unmodified PMMA-coated coverslips at 42 ± 1 ° compared to 75 ± 2 ° ($p = 2x10^{-6}$). Additionally, there was a significant increase in contact angle after azobenzene modification for MMAcoAEM-coated coverslips from 42 ± 1 ° to 71 ± 1 ° ($p = 2x10^{-7}$). After incubation in β-CD, the contact angle of azobenzene modified samples significantly increased from 71 ± 1 ° to 75 ± 1 ° (p = 0.002) while the angle of unmodified MMAcoAEM controls did not significantly change (p = 0.59).

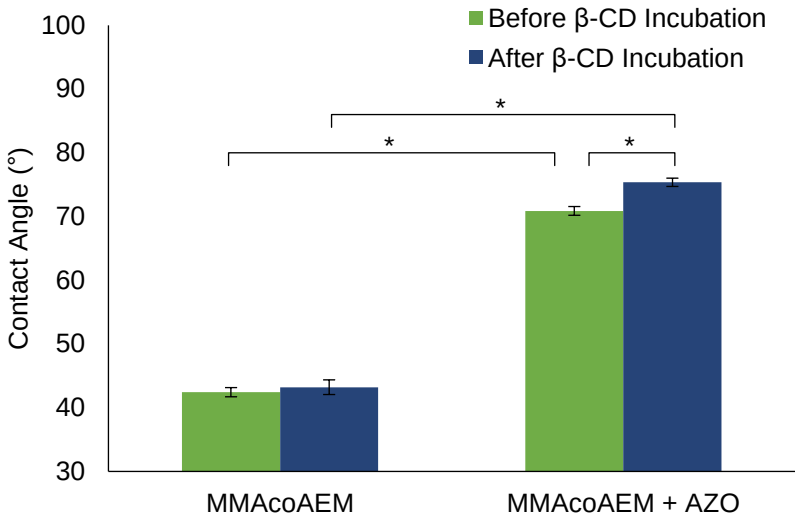

Figure 4.7: Static water contact angles for unmodified and azobenzene-modified (AZO) MMAcoAEM-coated coverslips before and after incubation with $1x10^{-3}$ M β-cyclodextrin (β-CD) in water with standard error bars. (n = 3).

4.3.5. Elemental analysis of MMAcoAEM via x-ray photoelectron spectroscopy

The surface chemistry of a MMAcoAEM-coated coverslip was determined by XPS, summarized in Table 4.8. The copolymer has a similar nitrogen content to amine-modified PMMA-coated coverslips, corroborating the similar ninhydrin results between the PMMA- and MMAcoAEM-coated coverslips.

Table 4.8: XPS results for MMAcoAEM-coated coverslips reported as Atomic Concentration (At %). (n = 1).

	MMAcoAEM Coated Coverslip	
	Position	At %
O 1s, C-O	533.94	12
O 1s, C=O	532.36	12.84
N 1s	400.25	0.26
C 1s, C=O	289.11	13.6
C 1s, C-O	286.93	12.72
C 1s, C-C	285.78	18.02
C 1s, CHx	285.05	29.96
Cl 2p1/2	201.73	0.01
Cl 2p3/2	199.6	0.02
Si 2p, O-Si-O	103.68	0.09
Si 2p O-Si-C	102.31	0.47

4.4. Photoresponsiveness of azobenzene-modified PMMA and MMAcoAEM

A summary of the azobenzene graft densities for modified samples is presented below.

Table 4.9: Summary of azobenzene (AZO) graft densities on functionalized PMMA (short spacer HMD, long spacer PPG-PEG-PPG) and MMAcoAEM surfaces with standard error. (n = 3)

Surface Modification	Azobenzene Group Density (nmol/cm^2)
HMD	
PMMA Disk	20.5 ± 0.4
PMMA-Coated Coverslip	3.4 ± 0.2
PPG-PEG-PPG	
PMMA Disk	2.2 ± 0.2
PMMA-Coated Coverslip	11.2 ± 2.6
MMAcoAEM	
MMAcoAEM-Coated Coverslip	18.1 ± 8.9
Bulk	24.8 ± 4.4

4.4.1. Photoisomerization studies using UV-VIS spectroscopy

To investigate the photoisomerization of azobenzene grafted to PMMA and MMAcoAEM surfaces, the surfaces were irradiated at 365 nm for 1 h using a 4 W UVL-21 compact UV lamp 5 cm from the sample surface. UV-VIS spectroscopy was used to measure the absorbance of native 4-(phenylazo)benzoic acid dissolved in solution and compare the photoisomerization curve to unmodified PMMA and azobenzene-modified coverslips at 30 minute intervals during irradiation.

There are apparent peaks at 326 nm and 440 nm corresponding to the $\pi - \pi^*$ *trans*- transmission band and n – π^* *cis*- transition band of azobenzene. As illustrated in Figure 4.8, the isomerization from *trans*- to *cis*- is measurable by a decrease in peak area at 326 nm and an increase in the peak at 440 nm after irradiation with 326 nm light. Comparatively, when β-CD binds to *trans*-azobenzene, azobenzene is shielded from absorbing UV-VIS light and the peak maxima at 326 nm and 440 nm both decrease. We hypothesize a similar process will be observed for azobenzene-modified surfaces.

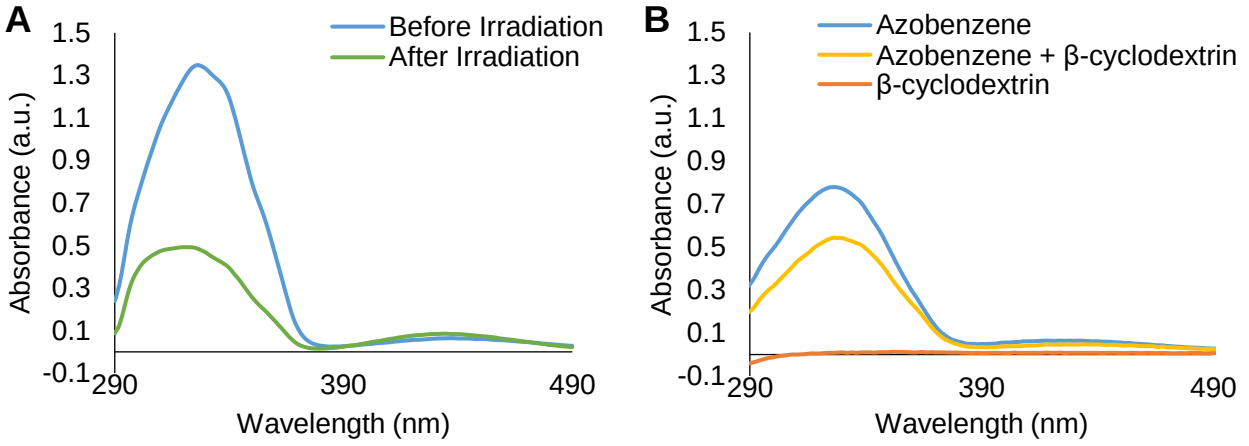

Figure 4.8: Absorbance of $1x10^{-4}$ M azobenzene in ethanol before and after 2 h irradiation with 365 nm light as in Figure 3.4 (A) and $1x10^{-3}$ M azobenzene and $1x10^{-3}$ M β-cyclodextrin in water before irradiation illustrating the shielding effect resulting from azobenzene-β-cyclodextrin complex formation (B).

The UV-VIS absorbance spectrum of PMMA-coated coverslips did not change shape after irradiation, however the curve shifted to lower values. This shift is hypothesized to be due to movement of the coverslip between readings, resulting in a change in baseline absorbance.

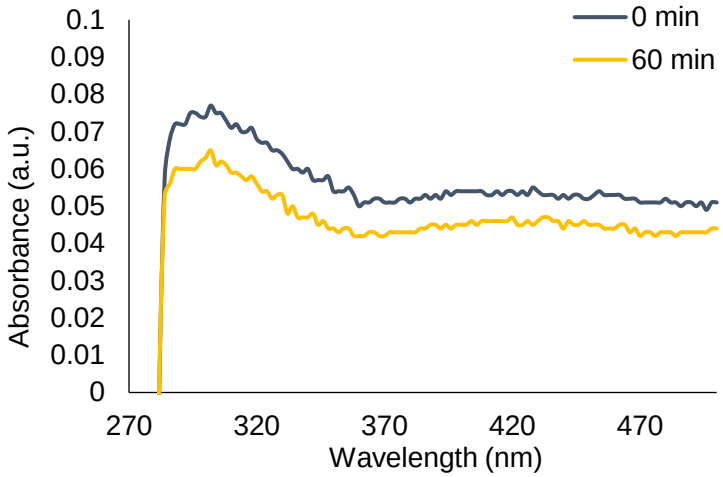

Figure 4.9: Photoisomerization study of PMMA-coated coverslip before and after irradiation with 365 nm light for 1 h with a 4 W UV lamp 5 cm from the sample surface.

Variability between coverslips resulted in slightly different baselines in each spectrum, so azobenzene curves were analyzed for general shape and absorption maxima. Coated coverslips were used for analysis as they were thin enough to measure UV-VIS through the material and were prepared using each modification method. Before irradiation, azobenzene-modified surfaces demonstrated a peak around 326 nm that was not present in amine controls, suggesting a successful modification. After irradiation for 1 h with 365 nm light, there were noticeable decreases in the peaks at 326 nm for each azobenzene-modified sample and negligible difference in the PPG-PEG-PPG and MMAcoAEM control curves. PPG-PEG-PPG was modified with more azobenzene groups than HMD coverslips and illustrated the strongest photoisomerization curve. A β-CD incubation was then performed on the PPG-PEG-PPG-modified control and azobenzene-modified surfaces.

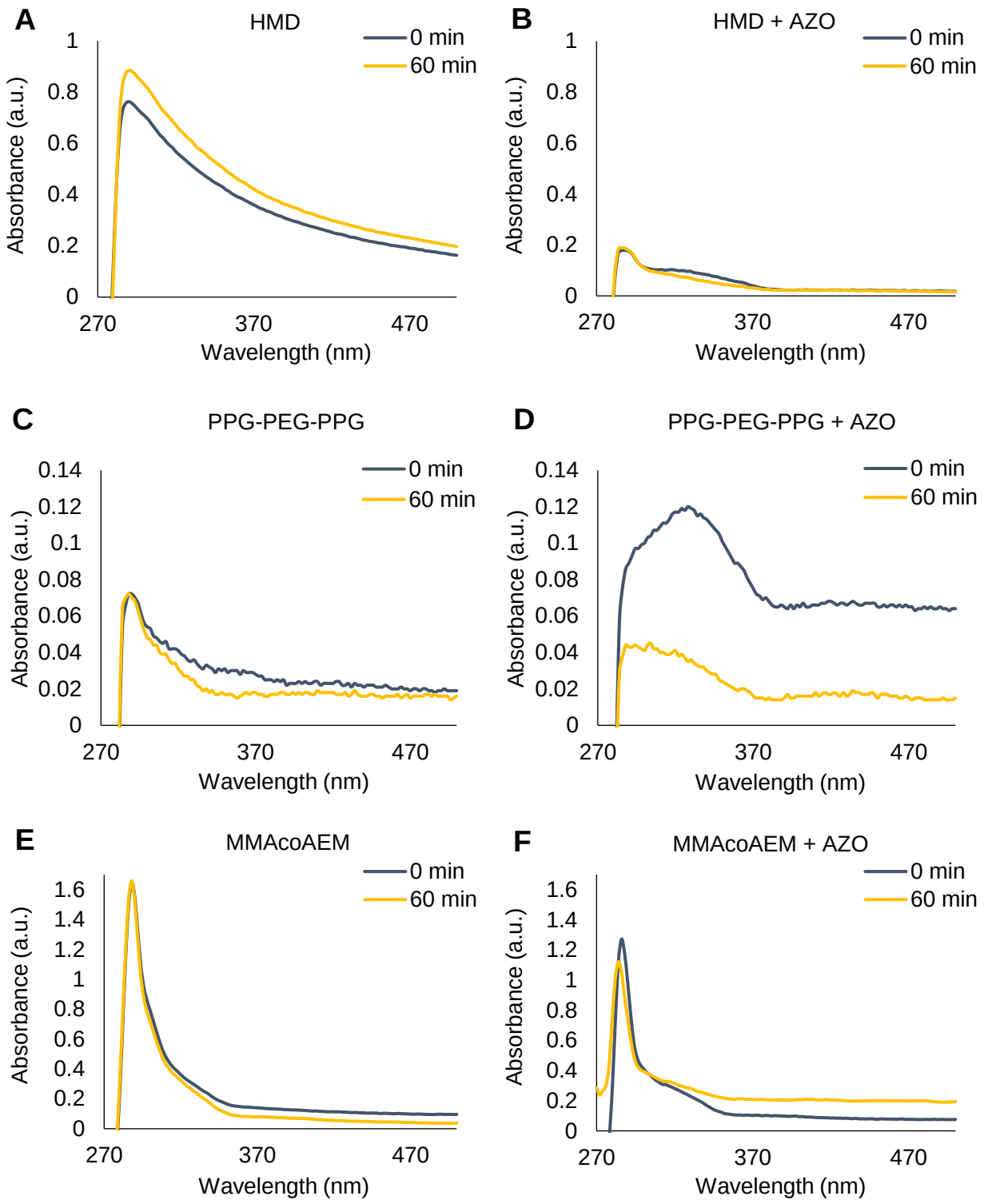

Figure 4.10: Photoisomerization study of HMD (A), HMD + AZO (B), PPG-PEG-PPG (C), PPG-PEG-PPG + AZO (D), MMAcoAEM (E), and MMAcoAEM + AZO (F) coverslips before and after 365 nm irradiation for 1 h with a 4 W UV lamp 5 cm from the sample surface. A distinct peak in azobenzene-containing samples at 326 nm suggests azobenzene is present at the surface.

PPG-PEG-PPG surfaces with and without azobenzene were incubated in 1 x 10^{-3} M β-CD in Millipore water for 1 h. To test whether β-CD formed a complex with azobenzene on the surface, the absorbance was measured at 30 min intervals during irradiation with 365 nm light. The azobenzene-modified PPG-PEG-PPG surface (Figure 4.11 B) showed a strong peak at 326 nm which decreased with increasing irradiation time, however the peak height at 0 min was lower than samples that had not been incubated in β-CD, suggesting β-CD is complexed with azobenzene. Further studies measuring the residual β-CD in solution are required to verify this finding.

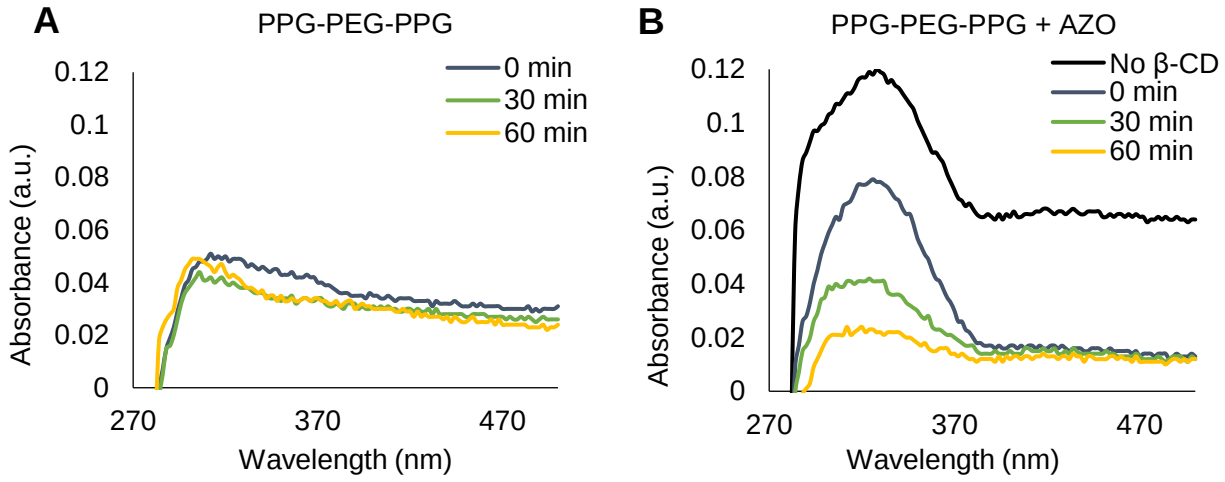

Figure 4.11: Photoisomerization study of PPG-PEG-PPG-modified (A) and azobenzene-modified (B) PMMA-coated coverslip after a 1 h incubation in a 1 x 10^{-3} M β-cyclodextrin solution. The spectrum of PPG-PEG-PPG + AZO without irradiation prior to β-CD incubation is also included in (B). Samples were irradiated with 365 nm light for 1 h using a 4 W UV lamp at 5 cm from the sample surface and absorbance measured and fresh water replenished at 30 min intervals.

4.5. HL-60 behaviour when incubated on functionalized PMMA surfaces

HL-60 cells were cultured with rough, smooth, and PMMA disks functionalized with amine and carboxyl groups to study the effects of PMMA surface chemistry on HL-60 cell viability and formation of extracellular traps (ETs). Tissue culture polystyrene (TCPS) was used as a control and cells were stimulated by phorbol 12-myristate 13-acetate (PMA) to induce differentiation and

promote adhesion to the growth surface. Cell viability was analyzed using an alamarBlue® assay and intracellular and extracellular deoxyribonucleic acid (DNA) stained using NucBlue® and SYTOX® green stains.

4.5.1. HL-60 cell adhesion and viability on PMMA of different chemistry

PMMA disks were smoothed to control for variations in roughness. Control studies showed no large differences in adhesion or viability on smooth or rough surfaces (Appendix B.1). More cells adhered onto TCPS and the functionalized PMMA with PMA (Figure 4.12 A) than without PMA (Figure 4.12 B). PMA was required to activate and promote the adherence of HL-60 cells onto surfaces, indicating that the materials themselves (or proteins adsorbed from medium to the materials) did not promote activation. There was a significantly lower number of live cells on amine-surfaces (10.2 cells/image) compared to PMMA (20.2 cells/image) ($p = 0.0005$) and carboxyl-functionalized PMMA (26.1 cells/image) ($p = 0.002$). The live cell count on carboxyl-functionalized samples were higher than on unmodified samples, but were not significantly different.

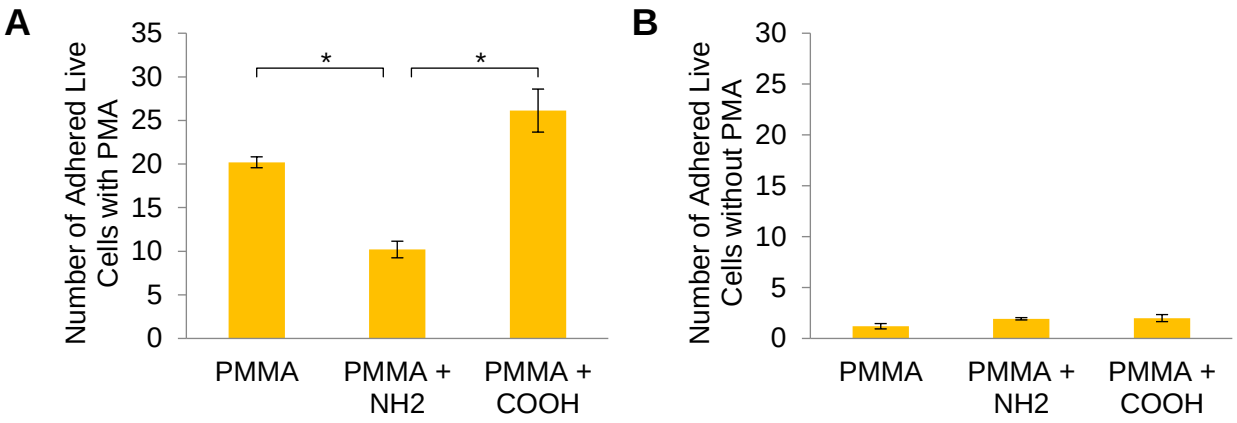

Figure 4.12: Number of live cells stained with NucBlue® on smooth unmodified (PMMA), HMD-modified (PMMA + NH2), and carboxyl-modified (PMMA + COOH) disks with (A) and without (B) incubation in PMA. There are no significant differences between samples without PMA. ($n = 3$, $*p < 0.005$).

The alamarBlue® assay assessed viability of HL-60s incubated with the different PMMA disks. The alamarBlue® ratio significantly decreased from 1.4 for smooth PMMA to 0.9 for carboxyl surfaces functionalized for 2 h ($p = 0.04$) or to 1.0 for carboxyl surfaces functionalized for 6 h ($p = 0.03$). The 48 h amine-functionalized surfaces also had a significantly higher viability than 2 h carboxyl ($p = 0.013$) or 6 h carboxyl ($p = 0.015$) functionalized surfaces.

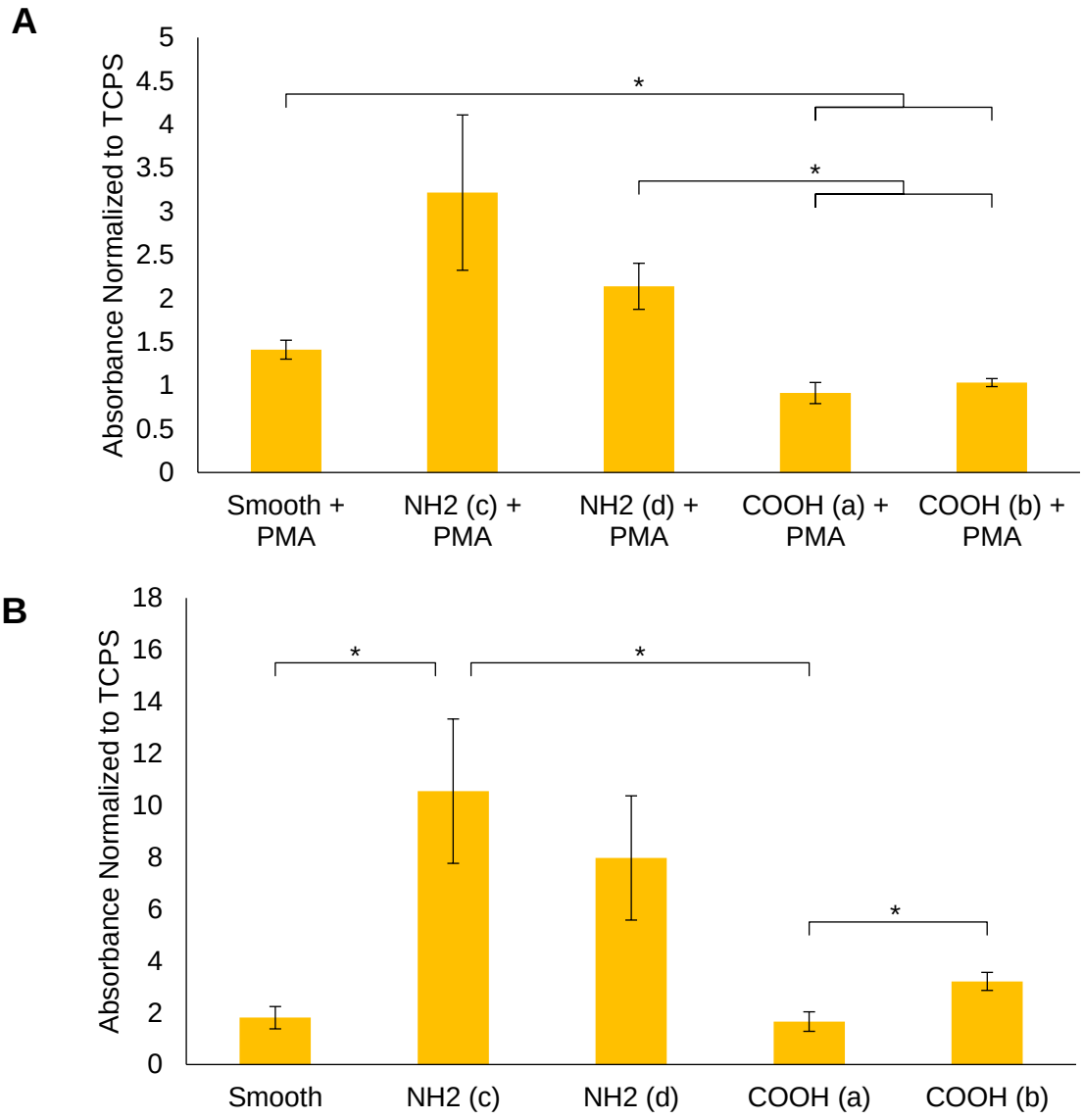

Figure 4.13: AlamarBlue® assay results normalized to TCPS + PMA (A) or TCPS (B). Results compare unmodified smooth PMMA disks to amine disks (NH2) modified in pH 12.5 sodium tetraborate buffer for 2 h (c) or 48 h (d) carboxyl disks (COOH) modified for 2 h (a) or 6 h (b). ($n = 3$, $*p < 0.05$).

For incubations without PMA, there was a significant increase in the alamarBlue® ratio from 1.7 to 3.2 for carboxyl surfaces functionalized for 6 h as opposed to 2 h in 6 N NaOH ($p = 0.04$). Comparatively, there was a significant decrease in the alamarBlue® ratio from 10.2 to 7.7 for amine surfaces functionalized for 48 h as opposed to 2 h at a pH of 12.5 ($p = 0.02$), indicating the number of grafted molecules at the surface may affect cell viability. The error bars on both amine samples are large compared to those of smooth and carboxyl modified PMMA disks, which may be contributing to the lack of significant differences between amine and other samples. However, the amine samples consistently show increased cell activity compared to TCPS and smooth and carboxyl modified PMMA disks for both inactivated and PMA-activated HL-60 cells.

4.5.2. Comparison of surface chemistry on the presence of extracellular DNA

To observe and compare live cells and cells that have released their DNA (likely as extracellular traps),[44] adhered cells on PMMA, amine-, and carboxyl-functionalized PMMA were dyed using NucBlue® and SYTOX® stains. The NucBlue® reagent permeates live cells to stain intracellular DNA blue while SYTOX® is unable to permeate cells and stains extracellular DNA or DNA in dead cells green. Cells undergoing cell death or releasing extracellular DNA traps (ETosis) appear as a mixture of the two colours. Representative images of unmodified, amine-modified, and carboxyl-modified PMMA are included in Figure 4.14.

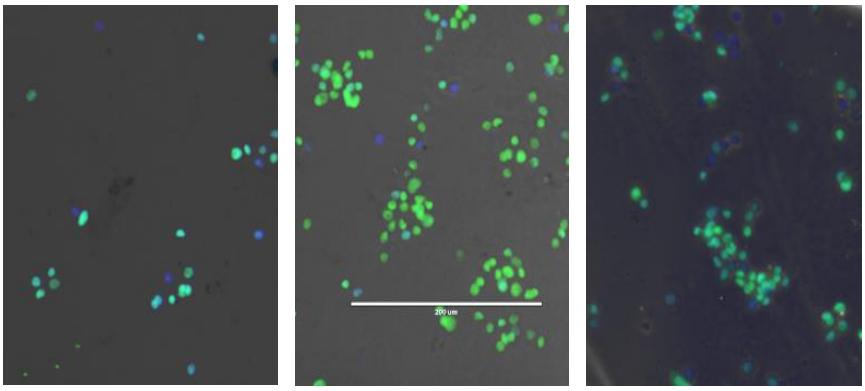

PMMA PMMA + NH_2 PMMA + COOH

Figure 4.14: Sample of NucBlue® (blue) and SYTOX® (green) stained smooth unmodified (PMMA), HMD-modified (PMMA + NH_2), and carboxyl-modified (PMMA + COOH) disks activated with PMA images at 20 times magnification. Scale bar is 200 μm.

The ratio of blue/green stained cells (ETosis/No ETosis) is summarized in Figure 4.15. HL-60 incubated with amine-functionalized surfaces (with PMA) have a significantly higher DNA staining ratio at 3.6 compared to 2.1 for PMMA ($p = 0.01$) and 1.5 for carboxyl-functionalized PMMA ($p = 0.04$). The difference between PMMA and PMMA-COOH is not significant ($p = 0.23$).

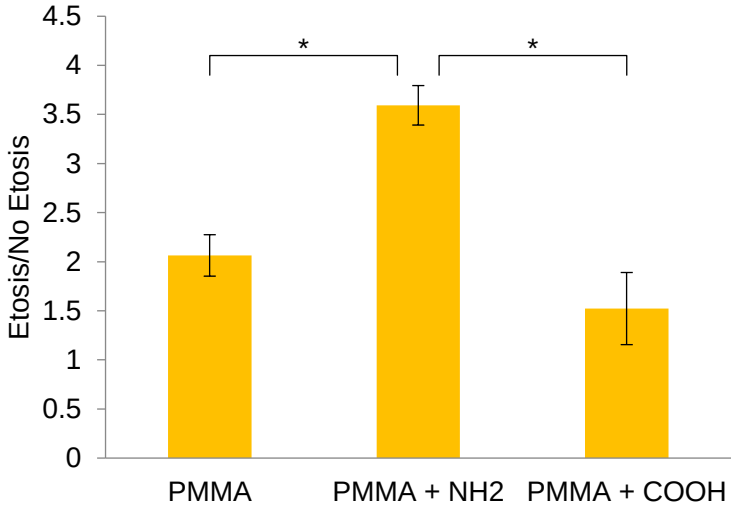

Figure 4.15: Ratio of green to blue stained cells seeded onto unmodified (PMMA), HMD-modified (PMMA + NH2), and carboxyl-modified (PMMA + COOH) disks with incubation in PMA. Dead cells stain green while live cells stain blue. Values reported are a mean of 15 representative images of each surface chemistry; 5 measurements per disk imaged. (n = 3).

Chapter 5. Discussion

Functionalization with amine or carboxyl groups and modification with azobenzene changed the hydrophilicity of poly(methyl methacrylate) (PMMA) and methyl methacrylate-co-2-aminoethyl methacrylate (MMAcoAEM) surfaces, illustrating wet chemical methods were successful in changing surface properties. One advantage of using modified PMMA for modification is that O,O'-bis(2-aminopropyl) propylene glycol-block-polyethylene glycol-block-polypropylene glycol (PPG-PEG-PPG) grafts provide a higher amount of mobility to attached azobenzene in comparison to hexamethylenediamine (HMD) modified or MMAcoAEM surfaces, improving the photoresponsive characteristics of the surface. In addition, there were improvements in the viability of PMA-activated human promyelocytic leukemia HL-60 cells when incubated with amine- and carboxyl-functionalized surfaces compared to incubations with unfunctionalized PMMA, illustrating that the surface properties of PMMA can be manipulated to alter cell responses to the material.

5.1. Functionalization of PMMA with amine or carboxyl groups was slightly improved over current methods

5.1.1. Coating with MMAcoAEM increased the density of amine groups at the surface compared to amine-functionalized PMMA coatings

PMMA disks and PMMA-coated coverslips were functionalized with NH_2 using aminolysis adapted from Fixe *et al.*[1] Strengthening the buffer from pH 11.5 to 12.5 caused a larger number of amine groups in solution to be protonated, promoting nucleophilic attack on the ester of PMMA and improving the final amine graft density.[135] Interestingly, the reaction at pH 11.5 for

2 h produced surfaces with 11.2 ± 3.9 nmol/cm^2 of HMD – a significantly higher value than 0.29 ± 0.02 nmol/cm^2 reported by Fixe *et al*. using similar conditions,[1] but in the same range obtained using similar reagents such as lithioamines (6.85 ± 0.60 nmol/cm^2 to 13 ± 5 nmol/cm^2).[62,63] Polymerization with amine-containing monomers[128,136,137] or other reaction mechanisms for functionalization[18,26,59,138] could be used to further improve the density of amine grafts. For example, up to 317 nmol/cm^2 of amine-containing chitosan has been grafted to polysulfone after ozone treatment,[138] much larger than densities achieved using aminolysis. However, a high graft density of photoresponsive molecules can lead to deactivation or dampening of the photoresponsive behaviour,[84,104] so the density of amine groups is likely appropriate for this research.

There was no significant difference between the number of HMD or PPG-PEG-PPG groups grafted to PMMA disks ($p = 0.09$) or PMMA-coated coverslips ($p = 0.81$), suggesting chain length does not have a significant impact on the aminolysis efficiency. Further analysis of the amine surfaces could be used to determine if the spacers bind to the surface multiple times, particularly the PPG-PEG-PPG spacer. Doubly-bound spacers would increase hydrophobicity without contributing to available sites for azobenzene functionalization. Poly(ethylene glycol) (PEG) and PEG-derived spacers have low toxicity and good biocompatibility and have previously been used for biomolecule and chromophore conjugation to polymers.[28,139–141] However, densely packed PEG chains decrease cell adhesion as a result of inhibited protein adsorption to the surface.[13,142] Conformation of the surface chains may also affect surface properties. For example, Suh *et al*. determined the contact angle of PEG surfaces can be increased from 57 ° to 81 ° by introducing PEG nanostructures >400 nm tall spaced 500 nm apart to the surface.[143]

The characterization of the MMAcoAEM samples may not have been representative of the bulk percentage of amine groups. The ninhydrin results contain a large amount of error and disagree with the ^{1}H NMR results, suggesting poor dispersity of amine groups in the bulk sample. Although simple, free-radical polymerization provides little control over molecular weight and homogeneity and is largely dependent on the reactivity ratios of the monomers used. Reactivity ratios (r) are used in copolymerizations to quantify the prevalence of monomers reacting with themselves (ratio >>1), equally reacting with the other monomer (r ~ 1), or their inability to react with themselves (r = 0) to predict copolymer structure. Higher ratios result in polymerization of individual monomers or a block-copolymer while lower reactivity ratios correspond to a random or alternating copolymer. ATRP polymerization can better control the polydispersity and molecular weight of methacrylate copolymers by monitoring conversion.[128,129] The reactivity ratio of MMA is higher in free-radical polymerization than in ATRP polymerization,[130] increasing the instances of homopolymerized chains of MMA. To our knowledge, the reactivity ratios for a copolymerization of MMA and AEM have not been calculated. However, free-radical copolymerizations of MMA with a similar monomer, 2-(dimethylamino)ethyl methacrylate (DMAEMA), have resulted in reactivity ratios of 0.72 for DMAEMA and 0.68 for MMA.[144] These values suggest that a DMAEMA and MMA copolymer would have a random or alternating copolymer structure and may be used to hypothesize that MMA and AEM copolymerization results in a similar copolymer structure. Future characterization of the MMAcoAEM copolymer should include repetition of the ^{1}H NMR results, comparison to the molecular weight, molecular weight distribution, glass transition temperature, tensile strength, and optical clarity of native and amine-functionalized PMMA.

5.1.2. Base-catalyzed hydrolysis functionalized PMMA similarly to other methods

The carboxyl functionalization produced similar results to literature, with PMMA functionalized with up to 211.8 ± 63.5 nmol/cm^2 carboxyl groups after a 1 h reaction in methanol and 6 N NaOH.[60,62] Previous studies have used concentrated sulfuric acid to achieve nearly 100 % conversion of PMMA ester groups to carboxyl groups in 1 h at 55 °C for isotactic PMMA and up to 85 % conversion for syndtactic PMMA at the same conditions.[61] Other groups have achieved a plateau at 240 ± 70 nmol/cm^2 after 20 min reacting in 6 M sulfuric acid.[62] Weaker acids, such as hydrochloric or hydroiodic acid, have also been coupled with a longer reaction time to hydrolyze the surface. The major drawback of using acid hydrolysis is that the surface can become etched, leading to variation between samples and a loss in transparency. Air plasma has also been used to functionalize PMMA with up to 210 ± 80 nmol/cm^2 carboxyl groups after 10 s of exposure.[62] However, extended treatment with plasma can further react the surface resulting in a decrease in carboxylic acid functionality and the formation of oxides, acid anhydride, and aldehyde groups.[62,145] Future studies could focus functionalization on isotactic or syndtactic PMMA to decrease reaction time, but ultimately, this method of carboxyl functionalization successfully altered the PMMA surface properties in a controlled manner while using less damaging reagents than other conventional methods.

5.1.3. Improvements to PMMA functionalization and measurements

The distribution of groups at the surface is primarily driven by concentration gradients for wet chemical methods and could be better controlled using polymerization, grafting-to, or reaction stages with protective groups. Modifying individual samples also introduces variability sample-to-sample and between controls, appearing as error in the ninhydrin and contact angle

results. Additionally, this method adds significantly less functionality to the surface than polymerized materials however populating the surface with functional groups will impact the cell response to the material. Still, this method selectively modifies the surface and allows simpler purification of the final material than bulk modification or polymerization.

An important consideration for the development of surfaces is that it is difficult to measure small concentrations of molecules at the surface accurately. Contamination is easy and samples for XPS and contact angle measurements must be handled carefully to ensure measurements are accurately depicting the surface. Difficulties also arose characterizing surfaces with XPS due to sample-to-sample variability, ensuring all solvent/water was eluted from samples, and minimizing the curvature of polymer surfaces. The ninhydrin and titration chemical assays were the most useful for quantifying the amine and carboxyl reactions, however both quantification methods had a large amount of error. This could be due to the variation in surface arrangement between samples, the number of samples tested, or the sensitivity of the method used. The ninhydrin assay may also have been providing inconsistent quantification due to penetration of the dye molecules into the bulk sample. Absorbance measurements only accounted for Ruhemann's purple free-floating in solution and overlooked any dye trapped in the fluid-adsorbing outer layer of the polymer. This effect was observed in few samples and measurements from these samples were excluded from final graft density calculations. Moving forward, modifications using fluorescently tagged functional groups could be used to corroborate the extent of PMMA functionalization. Though there were statistically significant differences between contact angles of unmodified, amine, carboxyl, and azobenzene surfaces, changes of less than 10 ° may not be biologically significant and require testing with cells. Additional quantification techniques such as

scanning electron microscopy (SEM) and surface plasmon resonance (SPR) may also be used to support the elemental composition of the surfaces determined using XPS.

5.2. Azobenzene attached to PMMA coatings retained the ability to photoisomerize

Azobenzene showed the ability to photoisomerize when attached to PMMA-coated coverslips, in agreement with literature.[74,85,91] The photoresponsiveness of main and side chain azobenzene grafts has previously been explored by Ding and colleagues through the study of linear, graft, and comb azo-containing polymers.[74] In that study, there were no changes to absorbance wavelength between the linear and graft copolymer, however the isomerization efficiency of the main-chain azobenzene was deemed significantly lower than side-chain azobenzene based on the times of isomerization.[74] Interestingly, the comb azo-polymer demonstrated complex isomerization based on whether the main- or side-chains first isomerized to the *cis*- structure.

In our studies, a stronger photoisomerization signal was observed in samples with the longer PPG-PEG-PPG spacer. This may be due to improvements in photoisomerization efficiency with increased mobility provided by a long spacer. To study the effects of steric hindrance on photoisomerization, Kolpak *et al*. developed azobenzene-modified nanotubes as high energy density storage for thermal energy.[146] They found that repulsive interactions dominate the behaviour of *cis*- isomers separated by less than 6 Å, decreasing isomerization efficiency. Above this separation distance, the energy required to photoisomerize generally increased with separation distance for the *cis*- isomer, however the *trans*- isomer was not greatly affected by steric hindrance due to its planar nature.[146] Similarly, Haque *et al*. determined that increasing chain flexibility

improved the isomerization efficiency of azobenzene through free arrangement of the azobenzene groups into a parallel orientation.[85] Blends of PMMA and 40 wt% azobenzene have also produced very similar absorbance curves to freely dissolved azobenzene in solution, further illustrating that mobile azobenzene has a higher isomerization efficiency.[75] Thus, azobenzene with a larger range of motion or less steric hindrance can photoisomerize more easily, replicated in our results between the PPG-PEG-PPG (long spacer) and HMD or MMAcoAEM (short spacer).

5.3. Cyclodextrin complexation affected azobenzene absorbance

It is difficult to conclude whether β-cyclodextrin (β-CD) had a strong affinity for azobenzene bound to amine-functionalized PMMA and MMAcoAEM surfaces. As demonstrated with a trial in solution, the absorbance of azobenzene is decreased when it forms an inclusion complex in solution. A similar study by Bortolus and Monti indicated that with increasing cyclodextrin content in solution, the *trans*-azobenzene absorbance was decreased, however the *cis*-azobenzene spectrum was unaffected.[147] Additional studies have concluded that complexation between β-CD and *cis*-azobenzene may be observed, but is unfavoured and weaker than complexation with the *trans*- isomer.[81,148] A comparable effect was observed between the absorbance curves of the unmodified PMMA and PPG-PEG-PPG controls (no azobenzene) before and after adding β-CD, with a change observed in both the *trans*- and *cis*- absorbance. This finding could correspond to non-specific adsorption of β-CD to PMMA or inclusion complex formation between β-CD and both *trans*- and *cis*-azobenzene. It is also possible that PPG-PEG-PPG chains may have interacted with the hydrophobic cavity of β-CD due to end group hydrophobicity or chain mobility/length, similar to β-CD interactions with hydrocarbon chains observed in literature.[107,149]

The contact angle and photoisomerization results should be complemented with quantitative analysis of the β-CD groups on each surface by using a fluorescently labelled β-CD. Additionally, surfaces should be investigated for changes in physical properties after irradiation to determine if the *trans*- to *cis*- isomerization results in significantly different surface properties[150] and whether β-CD detaches from the surface after irradiation.

5.4. Applications of azobenzene surfaces for biomedical research

Our focus was developing a generic, covalently modified polymer with photoswitchable surface properties. Azobenzene has been previously used to develop photoswitchable surfaces as copolymers,[90] SAMs,[101] and relief gratings.[76] Auernheimer *et al*. developed a photoswitchable peptide by modifying arginine-glycine-aspartate (RGD) with an azobenzene moiety, then coating the material onto PMMA to control cell adhesion.[29] Stemming from this work, Liu *et al*. investigated SAMs containing a mixture of a similar RGD-azobenzene to promote adhesion and PEG oligomers to inhibit non-specific cell adhesion, observing a similar result.[30] With 0.1% only the alkanethiols on the surface modified with azobenzene, specific cell adhesion to the *trans*-isomer was demonstrated.[30] An important consideration in the development of these photoswitchable surfaces is how the technology will be implemented *in vivo*. Azopolymers are capable of retaining surface patterns in aqueous environments,[151] and visible light has been used to remove patterns using 15 mW, 488 nm irradiation for 2 min in the presence of cells without affecting cell viability.[73] Our experiments utilized a much higher power UV lamp to achieve photoisomerization of azobenzene-modified surfaces. Further development of these materials for *in vivo* applications requires the surfaces to photoisomerization using lower power UV irradiation to minimize damage to surrounding cells.[73]

5.5. HL-60 cell culture on amine- and carboxyl-functionalized PMMA disks

Cell differentiation, adherence, and viability were also affected by changing surface properties. Roughness is known to affect cell proliferation, orientation, and migration differently for different cell types. Increased surface roughness also initiates non-apoptotic cell death of neutrophils via their release of reactive oxygen species.[14] To maximize cell viability smooth PMMA was used to culture HL-60 cells. There was no indication that roughness affected the efficiency of the functionalization procedures.

Charge, hydrophilicity, and quantity of surface functional groups also play a role in the cellular response to a material. Increasing surface wettability has been shown to improve cell adhesion,[15] with some studies observing optimal adhesion in the 40 ° – 60 ° range.[15,16] In agreeance with literature, adding carboxyl or amine groups to smoothed PMMA increased wettability and decreased the contact angle significantly from 76 ± 1 ° to 42 ± 6 ° or 66 ± 2 ° respectively.[16,62]

AlamarBlue® assays and DNA staining were used to infer HL-60 cell viability and behaviour on PMMA and functionalized PMMA surfaces. The alamarBlue® assay indicated that adding hydrophilic groups to the surface resulted in higher cell viability with both amine and carboxyl surfaces, however positively charged groups provided the highest increase in viability. Despite a lower count of live cells on the surfaces of aminated PMMA, there was an increase in cell activity.

Although viability and proliferation were studied, the effect of surface chemistry on the type of HL-60 cell differentiation with PMA was not investigated. PMA is believed to initiate

differentiation of HL-60 cells into a macrophage/monocyte-like phenotype while promoting adhesion.[50,51] Without knowledge of the phenotype of activated HL-60 cells, it is difficult to conclude how the surface chemistry impacts cell behaviour. Particularly of interest to this study was the noted increase in extracellular DNA for HL-60 cells incubated with amine-functionalized PMMA, hypothesized to be a result of the formation of extracellular traps (ETosis). The release of DNA and chromatin to form extracellular traps (ETs) has been attributed to neutrophil response to acute inflammation but recent evidence has shown the formation of ETs from monocytes.[45] Based on the findings of increased extracellular DNA found on amine-functionalized samples, the presence of amine groups promotes ETosis compared to native or carboxyl-functionalized PMMA. Further evidence is required to determine whether the phenotype of HL-60 cells was affected by surface chemistry and to identify the extracellular DNA stained as NETs or ETs. Further investigation into the cell morphology and behaviour of PMA-differentiated HL-60 cells may be achieved by using antibody stains to detect the presence of neutrophil- or macrophage-like cell attributes. Extracellular traps may be identified using citrullinated Histone H3[43,152] or neutrophil elastase,[42,153] neutrophils may be identified using CD66b antibodies,[154] and monocytes/macrophages may be identified using the monoclonal antibody MAS 072.[155]

Chapter 6. Conclusions and future work

6.1. Azobenzene grafted to functionalized PMMA generated a photoresponsive surface

In this work, wet chemical modification was used to modify the surface of poly (methyl methacrylate) (PMMA) disks and coatings on glass coverslips with azobenzene moieties. Smoothed PMMA surfaces were functionalized with amine or carboxyl groups, with amine-functionalized surfaces later modified with azobenzene using carbodiimide chemistry. The amine functionalization was optimized by increasing the pH to 12.5 to increase the density of hexamethylenediamine (HMD) groups to 36.4 ± 5.7 nmol/cm^2 from 0.3 ± 0.02 nmol/cm^2 previously reported in literature.[1] Base-catalyzed hydrolysis was used to achieve a carboxyl surface density of 211.8 ± 63.5 nmol/cm^2. In addition, coatings of a synthesized copolymer of methyl methacrylate (MMA) with 0.7 mol% 2-aminoethyl methacrylate (AEM) (copolymer MMAcoAEM) had twice the number of amine groups available for modification as amine-functionalized PMMA. This copolymer shows promise as a coating material to introduce positively charged, hydrophilic groups to hydrophobic polymers and may be used to study cell-material interactions alongside functionalized polymers or charged copolymers, such as methyl methacrylate-co-methacrylic acid (MMAcoMAA).

Azobenzene surfaces can be used to achieve reversible, patternable surface modifications to a range of polymeric surfaces. Although relatively new to biomedical applications, azobenzene surfaces have potential to be used for interactive cell scaffolds, diagnostic tools, and ocular devices such as intraocular lenses (IOLs). Amine-functionalized PMMA and the MMAcoAEM copolymer were modified with 20.5 ± 0.4 nmol/cm^2 (HMD),

11.2 ± 2.6 nmol/cm^2 (PPG-PEG-PPG), or 24.8 ± 4.4 nmol/cm^2 (MMAcoAEM) of azobenzene. Azobenzene-modified surfaces showed significant differences from amine-functionalized controls in the ninhydrin assay, contact angle, and ultraviolet-visible (UV-VIS) photoisomerization studies, suggesting the modifications were successful. Importantly, the surfaces with grafted azobenzene illustrated UV-VIS absorbance curves similar to azobenzene dissolved in ethanol, verifying immobilized azobenzene retained the ability to photoisomerize after attachment to the surface. Furthermore, β-cyclodextrin (β-CD) incubation significantly altered the photoisomerization of azobenzene-modified PPG-PEG-PPG surfaces, indicating that bound azobenzene was capable of complexing with β-CD. This feature of the material allows for further customization of properties using biomolecules or functional groups conjugated to β-CD.

Amine and carboxyl-functionalized surfaces were also used for HL-60 cell culture to determine how changing the surface properties may affect the cellular response to the material. AlamarBlue® assays and deoxyribonucleic acid (DNA) staining indicated that adding amine or carboxyl groups to the surface resulted in different cell behaviour compared to unfunctionalized PMMA. There were fewer live cells on amine-functionalized samples, however those surfaces also promoted higher cell activity and more extracellular DNA than unfunctionalized or carboxyl-functionalized PMMA. Amine-functionalized surfaces also contained the highest amount of extracellular DNA, suggesting surface chemistry may influence HL-60 cell differentiation and the release of extracellular traps (ETs).

6.2. Future work

The complete characterization of the copolymer MMAcoAEM should be addressed in future studies as this work only investigated the number of amine groups available for reaction. Characterization of this polymer should include additional NMR studies and investigation of thermal properties using thermogravimetric analysis or differential scanning calorimetry to infer the purity and structure of the copolymer. Gel permeation chromatography may also be used to determine the molecular weight and polydispersity of the copolymer to ensure batch-to-batch homogeneity and for comparison to other polymers including PMMA.

The effects of grafting azobenzene on its isomerization kinetics were not studied in this work. Future work should investigate the reversibility of the photoisomerization of azobenzene-modified surfaces by cycling between irradiation at 326 nm and 440 nm. This process will give insight into the dynamics of grafted azobenzene, whether the efficiency of isomerization was affected by attaching azobenzene to surfaces, and how the tether length and flexibility may play a role.

In addition, the changes to surface properties with azobenzene in the *trans*- and *cis*-conformations should be investigated. Switching the surface properties of materials with light could be used to modulate the behaviour of cells grown on the surface. First, the cytotoxicity of azobenzene- and β-CD-modified surfaces should be evaluated by culturing cells on the surfaces and measuring cell viability. Secondly, the cell reaction to *trans*- to *cis*- isomerization of azobenzene, the release of β-CD from the surface, and functional groups on the surface could be monitored by measuring adhered cells, viability, and gene expression.

Finally, surface patterning of the azobenzene surfaces could be investigated by using photomasks to controllably irradiate portions of the surface. Our studies did not fully investigate the reversible attachment of β-CD to azobenzene surfaces, however further alteration of surface properties could be explored by modifying β-CD with peptide or nucleic acid chains before incubation with the azobenzene surface. In combination, these methods could be used to pattern a surface with different biomolecules to study the effect on surface properties and cell-material interactions.

Bibliography

1. Fixe, F., Dufva, M., Telleman, P. & Christensen, C. B. V. Functionalization of poly(methyl methacrylate) (PMMA) as a substrate for DNA microarrays. *Nucleic Acids Res.* **32,** 1–8 (2004).
2. dos Santos, V., Brandalise, R. N. & Savaris, M. Biomaterials: Characteristics and Properties. in *Engineering of Biomaterials* 5–15 (Springer, Cham, 2017). doi:10.1007/978-3-319-58607-6_2
3. Anderson, J. M. Biological responses to materials. *Annu. Rev. Mater. Res.* **31,** 81–110 (2001).
4. Anderson, J. M., Rodriguez, A. & Chang, D. T. Foreign Body Reaction to Biomaterials. *Semin. Immunol.* **20,** 86–100 (2008).
5. Lanza, R., Langer, R. & Vacanti, J. P. *Principles of Tissue Engineering*. (Academic Press, 2013).
6. Kang, I.-K., Kwon, B. K., Lee, J. H. & Lee, H. B. Immobilization of proteins on poly (methyl methacrylate) films. *Biomaterials* **14,** 787–792 (1993).
7. Nelson, G. W., Perry, M., He, S.-M., Zechel, D. L. & Horton, J. H. Characterization of covalently bonded proteins on poly(methyl methacrylate) by X-ray photoelectron spectroscopy. *Colloids Surf. B Biointerfaces* **78,** 61–68 (2010).
8. Fixe, F., Dufva, M., Telleman, P. & Christensen, C. B. V. One-step immobilization of aminated and thiolated DNA onto poly(methylmethacrylate) (PMMA) substrates. *Lab. Chip* **4,** 191–195 (2004).

9. Opitz, J. *et al.* Site-specific binding and stretching of DNA molecules at UV-light-patterned aminoterpolymer films. *Nanotechnology* **15,** 717–723 (2004).

10. Krall, E. M. *et al.* Intraindividual aqueous flare comparison after implantation of hydrophobic intraocular lenses with or without a heparin-coated surface. *J. Cataract Refract. Surg.* **40,** 1363–1370 (2014).

11. Wang, B. *et al.* Surface modification of intraocular lenses with hyaluronic acid and lysozyme for the prevention of endophthalmitis and posterior capsule opacification. *RSC Adv* **5,** 3597–3604 (2015).

12. Lin, Q. *et al.* Hydrated polysaccharide multilayer as an intraocular lens surface coating for biocompatibility improvements. *J Mater Chem B* **3,** 3695–3703 (2015).

13. Pei, J., Hall, H. & Spencer, N. D. The role of plasma proteins in cell adhesion to PEG surface-density-gradient-modified titanium oxide. *Biomaterials* **32,** 8968–8978 (2011).

14. Chang, S., Popowich, Y., Greco, R. S. & Haimovich, B. Neutrophil survival on biomaterials is determined by surface topography. *J. Vasc. Surg.* **37,** 1082–1090 (2003).

15. Lim, J. Y. *et al.* Osteoblast adhesion on poly(L-lactic acid)/polystyrene demixed thin film blends: effect of nanotopography, surface chemistry, and wettability. *Biomacromolecules* **6,** 3319–3327 (2005).

16. Arima, Y. & Iwata, H. Effect of wettability and surface functional groups on protein adsorption and cell adhesion using well-defined mixed self-assembled monolayers. *Biomaterials* **28,** 3074–3082 (2007).

17. Puleo, D. A., Holleran, L. A., Doremus, R. H. & Bizios, R. Osteoblast responses to orthopedic implant materials in vitro. *J. Biomed. Mater. Res.* **25,** 711–723 (1991).

18. Chua, K.-N. *et al.* Functional nanofiber scaffolds with different spacers modulate adhesion and expansion of cryopreserved umbilical cord blood hematopoietic stem/progenitor cells. *Exp. Hematol.* **35,** 771–781 (2007).
19. Zhu, Y., Gao, C., He, T. & Shen, J. Endothelium regeneration on luminal surface of polyurethane vascular scaffold modified with diamine and covalently grafted with gelatin. *Biomaterials* **25,** 423–430 (2004).
20. Mukherjee, R., Chaudhury, K., Das, S., Sengupta, S. & Biswas, P. Posterior capsular opacification and intraocular lens surface micro-roughness characteristics: An atomic force microscopy study. *Micron* **43,** 937–947 (2012).
21. Huang, X.-D., Yao, K., Zhang, Z., Zhang, Y. & Wang, Y. Uveal and capsular biocompatibility of an intraocular lens with a hydrophilic anterior surface and a hydrophobic posterior surface. *J. Cataract Refract. Surg.* **36,** 290–298 (2010).
22. Zhang, J. & Han, Y. Active and responsive polymer surfaces. *Chem. Soc. Rev.* **39,** 676–693 (2010).
23. Ercole, F., Davis, T. P. & Evans, R. A. Photo-responsive systems and biomaterials: photochromic polymers, light-triggered self-assembly, surface modification, fluorescence modulation and beyond. *Polym Chem* **1,** 37–54 (2010).
24. Yoshizato, K., Takezawa, T. & Mori, Y. Cell Culture on a Thermo-Responsive Polymer Surface. *Nat. Biotechnol.* **8,** 854–856 (1990).
25. Boehm, D. A., Gottlieb, P. A. & Hua, S. Z. On-chip microfluidic biosensor for bacterial detection and identification. *Sens. Actuators B Chem.* **126,** 508–514 (2007).

26. Cheng, J.-Y., Wei, C.-W., Hsu, K.-H. & Young, T.-H. Direct-write laser micromachining and universal surface modification of PMMA for device development. *Sens. Actuators B Chem.* **99,** 186–196 (2004).

27. Gu, W.-X. *et al.* Construction of stable polymeric vesicles based on azobenzene and beta-cyclodextrin grafted poly(glycerol methacrylate)s for potential applications in colon-specific drug delivery. *Chem Commun* **51,** 4715–4718 (2015).

28. Chiang, C.-Y. & Chu, C.-C. Synthesis of photoresponsive hybrid alginate hydrogel with photo-controlled release behavior. *Carbohydr. Polym.* **119,** 18–25 (2015).

29. Auernheimer, J., Dahmen, C., Hersel, U., Bausch, A. & Kessler, H. Photoswitched Cell Adhesion on Surfaces with RGD Peptides. *J. Am. Chem. Soc.* **127,** 16107–16110 (2005).

30. Liu, D., Xie, Y., Shao, H. & Jiang, X. Using Azobenzene-Embedded Self-Assembled Monolayers To Photochemically Control Cell Adhesion Reversibly. *Angew. Chem. Int. Ed.* **48,** 4406–4408 (2009).

31. Keselowsky, B. G., Collard, D. M. & García, A. J. Integrin binding specificity regulates biomaterial surface chemistry effects on cell differentiation. *Proc. Natl. Acad. Sci.* **102,** 5953–5957 (2005).

32. Vroman, L. & Adams, A. L. Identification of rapid changes at plasma–solid interfaces. *J. Biomed. Mater. Res. A* **3,** 43–67 (1969).

33. Vroman, L. & Adams, A. L. Findings with the recording ellipsometer suggesting rapid exchange of specific plasma proteins at liquid/solid interfaces. *Surf. Sci.* **16,** 438–446 (1969).

34. Vogler, E. A. Structure and reactivity of water at biomaterial surfaces. *Adv. Colloid Interface Sci.* **74,** 69–117 (1998).

35. Kumar, N., Parajuli, O., Gupta, A. & Hahm, J. Elucidation of Protein Adsorption Behavior on Polymeric Surfaces: Toward High-Density, High-Payload Protein Templates. *Langmuir* **24,** 2688–2694 (2008).

36. Hasegawa, M. & Kitano, H. Adsorption kinetics of proteins onto polymer surfaces as studied by the multiple internal reflection fluorescence method. *Langmuir* **8,** 1582–1586 (1992).

37. Young, B. R., Pitt, W. G. & Cooper, S. L. Protein adsorption on polymeric biomaterials I. Adsorption isotherms. *J. Colloid Interface Sci.* **124,** 28–43 (1988).

38. Schmidt, D. R., Waldeck, H. & Kao, W. J. Protein Adsorption to Biomaterials. in *Biological Interactions on Materials Surfaces* 1–18 (Springer, 2009). doi:10.1007/978-0-387-98161-1_1

39. Goddard, J. M. & Hotchkiss, J. H. Polymer surface modification for the attachment of bioactive compounds. *Prog. Polym. Sci.* **32,** 698–725 (2007).

40. Vyner, M. C., Liu, L., Sheardown, H. D. & Amsden, B. G. The effect of elastomer chain flexibility on protein adsorption. *Biomaterials* **34,** 9287–9294 (2013).

41. Henson, P. M. The Immunologic Release of Constituents from Neutrophil Leukocytes: II. Mechanisms of Release During Phagocytosis, and Adherence to Nonphagocytosable Surfaces. *J. Immunol.* **107,** 1547–1557 (1971).

42. Brinkmann, V., Laube, B., Abu Abed, U., Goosmann, C. & Zychlinsky, A. Neutrophil Extracellular Traps: How to Generate and Visualize Them. *J. Vis. Exp. JoVE* (2010). doi:10.3791/1724

43. Remijsen, Q. *et al.* Dying for a cause: NETosis, mechanisms behind an antimicrobial cell death modality. *Cell Death Differ.* **18,** 581–588 (2011).

44. Goldmann, O. & Medina, E. The expanding world of extracellular traps: not only neutrophils but much more. *Front. Immunol.* **3,** 1–10 (2012).

45. Granger, V. *et al.* Human blood monocytes are able to form extracellular traps. *J. Leukoc. Biol.* **102,** 775–781 (2017).

46. Pintwala, R., Postnikoff, C., Molladavoodi, S. & Gorbet, M. Coculture with intraocular lens material-activated macrophages induces an inflammatory phenotype in lens epithelial cells. *J. Biomater. Appl.* **29,** 1119–1132 (2015).

47. Collins, S. J. The HL-60 Promyelocytic Leukemia Cell Line: Proliferation, Differentiation, and Cellular Oncogene Expression. *J. Am. Soc. Hematol.* **70,** 1233–1244 (1987).

48. Hauert, A. B., Martinelli, S., Marone, C. & Niggli, V. Differentiated HL-60 cells are a valid model system for the analysis of human neutrophil migration and chemotaxis. *Int. J. Biochem. Cell Biol.* **34,** 838–854 (2002).

49. Birnie, G. D. The HL60 cell line: a model system for studying human myeloid cell differentiation. *Br. J. Cancer. Suppl.* **9,** 41–45 (1988).

50. Rovera, G., Santoli, D. & Damsky, C. Human promyelocytic leukemia cells in culture differentiate into macrophage-like cells when treated with a phorbol diester. *Proc. Natl. Acad. Sci.* **76,** 2779–2783 (1979).

51. Lee, C. W., Sokoloski, J. A., Sartorelli, A. C. & Handschumacher, R. E. Induction of the differentiation of HL-60 cells by phorbol 12-myristate 13-acetate activates a Na+-dependent uridine-transport system. Involvement of protein kinase C. *Biochem. J.* **274,** 85–90 (1991).

52. Andersson, G. & Johansson, E. K. Adhesion of human myelomonocytic (HL-60) cells induced by 1,25-dihydroxyvitamin D3 and phorbol myristate acetate is dependent on

osteopontin synthesis and the alpha v beta 3 integrin. *Connect. Tissue Res.* **35,** 163–171 (1996).

53. Hoffman, A. S. Surface modification of polymers: physical, chemical, mechanical and biological methods. in *Macromolecular Symposia* **101,** 443–454 (Wiley Online Library, 1996).
54. Neoh, K.-G. Bioactive surface functionalization. *J. Appl. Polym. Sci.* **131,** 40607 (2014).
55. Fried, J. R. *Polymer Science and Technology*. (Prentice Hall Professional Technical Reference, 2003).
56. Nakajima, N. & Ikada, Y. Mechanism of amide formation by carbodiimide for bioconjugation in aqueous media. *Bioconjug. Chem.* **6,** 123–130 (1995).
57. Vashist, S. K. Comparison of 1-Ethyl-3-(3-Dimethylaminopropyl) Carbodiimide Based Strategies to Crosslink Antibodies on Amine-Functionalized Platforms for Immunodiagnostic Applications. *Diagnostics* **2,** 23–33 (2012).
58. Fischer, M. J. E. Amine Coupling Through EDC/NHS: A Practical Approach. in *Surface Plasmon Resonance* (eds. Mol, N. J. & Fischer, M. J. E.) **627,** 55–73 (Humana Press, 2010).
59. Lin, Y.-J., Tsai, B.-K., Tu, C.-J., Jeng, J. & Chu, C.-C. Synthesis of β-cyclodextrin and poly(amido amine) dendron click cluster and its synergistic binding property. *Tetrahedron* **69,** 1801–1807 (2013).
60. Patel, S., Thakar, R. G., Wong, J., McLeod, S. D. & Li, S. Control of cell adhesion on poly(methyl methacrylate). *Biomaterials* **27,** 2890–2897 (2006).
61. Semen, J. & Lando, J. B. The acid hydrolysis of isotactic and syndiotactic poly (methyl methacrylate). *Macromolecules* **2,** 570–575 (1969).

62. Brown, L., Koerner, T., Horton, J. H. & Oleschuk, R. D. Fabrication and characterization of poly(methylmethacrylate) microfluidic devices bonded using surface modifications and solvents. *Lab Chip* **6,** 66–73 (2006).

63. Henry, A. C. *et al.* Surface Modification of Poly(methyl methacrylate) Used in the Fabrication of Microanalytical Devices. *Anal. Chem.* **72,** 5331–5337 (2000).

64. Wei, Y. *et al.* Surface Modification of Hydrophobic PMMA Intraocular Lens by the Immobilization of Hydroxyethyl Methacrylate for Improving Application in Ophthalmology. *Plasma Chem. Plasma Process.* **31,** 811–825 (2011).

65. Latz, C. *et al.* Inhibition of lens epithelial cell proliferation by substituted PMMA intraocular lenses. *Graefes Arch. Clin. Exp. Ophthalmol.* **238,** 696–700 (2000).

66. Berges, C., Javakhishvili, I., Hvilsted, S., Sánchez, C. & Alcalá, R. Photoresponsive Azopolyester–PMMA Block Copolymers Obtained by Combination of ATRP, Polycondensation, and "Click" Chemistry. *Macromol. Chem. Phys.* **213,** 2299–2310 (2012).

67. Alidedeoglu, A. H., York, A. W., McCormick, C. L. & Morgan, S. E. Aqueous RAFT polymerization of 2-aminoethyl methacrylate to produce well-defined, primary amine functional homo- and copolymers. *J. Polym. Sci. Part Polym. Chem.* **47,** 5405–5415 (2009).

68. Ekpenyong, K. I. Monomer reactivity ratios: Acrylic acid-methylmethacrylate copolymerization in dimethylsulfoxide. *J Chem Educ* **62,** 173–174 (1985).

69. Sanfelice, R. C. *et al.* Hydrophobic methacrylic copolymers containing azobenzene moieties. *Polymer* **52,** 4703–4708 (2011).

70. Halacheva, S. S. *et al.* Injectable Biocompatible and Biodegradable pH-Responsive Hollow Particle Gels Containing Poly(acrylic acid): The Effect of Copolymer Composition on Gel Properties. *Biomacromolecules* **15,** 1814–1827 (2014).

71. Subbaraman, L. N., Glasier, M.-A., Senchyna, M., Sheardown, H. & Jones, L. Kinetics of *In Vitro* Lysozyme Deposition on Silicone Hydrogel, PMMA, and FDA Groups I, II, and IV Contact Lens Materials. *Curr. Eye Res.* **31,** 787–796 (2006).

72. Wang, B., Oleschuk, R. D., Petkovich, P. M. & Horton, J. H. Chemical force titrations of antigen- and antibody-modified poly(methylmethacrylate). *Colloids Surf. B Biointerfaces* **55,** 107–114 (2007).

73. Rianna, C. *et al.* Reversible Holographic Patterns on Azopolymers for Guiding Cell Adhesion and Orientation. *ACS Appl. Mater. Interfaces* **7,** 16984–16991 (2015).

74. Ding, L., Qiu, J., Li, J., Wang, C. & Wang, L. Novel Photoresponsive Linear, Graft, and Comb-Like Copolymers with Azobenzene Chromophores in the Main-Chain and/or Side-Chain: Facile One-Pot Synthesis and Photoresponse Properties. *Macromol. Rapid Commun.* **36,** 1578–1584 (2015).

75. Müller, M. *et al.* In situ atomic force microscopy studies of reversible light-induced switching of surface roughness and adhesion in azobenzene-containing PMMA films. *Appl. Surf. Sci.* **257,** 7719–7726 (2011).

76. Ubukata, T., Takahashi, K. & Yokoyama, Y. Photoinduced surface relief structures formed on polymer films doped with photochromic spiropyrans. *J. Phys. Org. Chem.* **20,** 981–984 (2007).

77. Cocchi, C., Moldt, T., Gahl, C., Weinelt, M. & Draxl, C. Optical properties of azobenzene-functionalized self-assembled monolayers: Intermolecular coupling and many-body interactions. *J. Chem. Phys.* **145,** 234701 1-10 (2016).

78. Bo, Q. & Zhao, Y. Fluorescence from an Azobenzene-Containing Diblock Copolymer Micelle in Solution. *Langmuir* **23,** 5746–5751 (2007).

79. Tang, X., Gao, L., Fan, X. & Zhou, Q. Controlled grafting of ethyl cellulose with azobenzene-containing polymethacrylates via atom transfer radical polymerization. *J. Polym. Sci. Part Polym. Chem.* **45,** 1653–1660 (2007).

80. Matencio, A., Hernández-García, S., García-Carmona, F. & Manuel López-Nicolás, J. An integral study of cyclodextrins as solubility enhancers of α-methylstilbene, a resveratrol analogue. *Food Funct.* **8,** 270–277 (2017).

81. Sanchez, A. M. & de Rossi, R. H. Effect of β-Cyclodextrin on the Thermal Cis- Trans Isomerization of Azobenzenes. *J. Org. Chem.* **61,** 3446–3451 (1996).

82. Angelini, G., Canilho, N., Emo, M., Kingsley, M. & Gasbarri, C. Role of Solvent and Effect of Substituent on Azobenzene Isomerization by Using Room-Temperature Ionic Liquids as Reaction Media. *J. Org. Chem.* **80,** 7430–7434 (2015).

83. Kyzio, J. B. & Frej, H. Substituent effects on physical properties of substituted azobenzenes. *Chem. Papers* **42,** 781–793 (1988).

84. Cocchi, C. & Draxl, C. Understanding the effects of packing and chemical terminations on the optical excitations of azobenzene-functionalized self-assembled monolayers. *J. Phys. Condens. Matter* **29,** 394005 1-12 (2017).

85. Haque, H. A., Hara, M., Nagano, S. & Seki, T. Photoinduced In-Plane Motions of Azobenzene Mesogens Affected by the Flexibility of Underlying Amorphous Chains. *Macromolecules* **46,** 8275–8283 (2013).

86. Takagishi, T., Katayama, A., Konishi, K. & Kuroki, N. The solubilities of azobenzene derivatives in water. *Kolloid-Z. Z. Für Polym.* **232,** 693–699 (1969).

87. Winkler, C. A., Halpern, J. & Brady, G. W. The Cis-Trans Isomerization of Azobenzene in Solution. *Can. J. Res.* **28,** 140–155 (1950).

88. Yang, C.-A., Wang, Q., Xie, H., Zhong, G. & Zhang, H. Synthesis and characterisation of polymethacrylates containing *para* -, *meta* - and *ortho* -monosubstituted azobenzene moieties in the side chain. *Liq. Cryst.* **37,** 1339–1346 (2010).

89. Brown, C. *et al.* Differential azobenzene solubility increases equilibrium cis/trans ratio in water. *J. Photochem. Photobiol. Chem.* **336,** 140–145 (2017).

90. Rianna, C., Ventre, M., Cavalli, S., Radmacher, M. & Netti, P. A. Micropatterned Azopolymer Surfaces Modulate Cell Mechanics and Cytoskeleton Structure. *ACS Appl. Mater. Interfaces* **7,** 21503–21510 (2015).

91. Weber, C. *et al.* Light-Controlled "Molecular Zippers" Based on Azobenzene Main Chain Polymers. *Macromolecules* **48,** 1531–1537 (2015).

92. Ube, T., Takado, K. & Ikeda, T. Photomobile Properties of Interpenetrating Polymer Network Films Composed of Azobenzene Liquid Crystalline Polymer and Polymethacrylates. *Mol. Cryst. Liq. Cryst.* **594,** 86–91 (2014).

93. Zhu, Y. & Wang, X. Synthesis and photoresponsive properties of two liquid crystalline polymers bearing branched azobenzene-containing side chains. *Polym. Chem.* **4,** 5108–5118 (2013).

94. Lambeth, R. H. & Moore, J. S. Light-Induced Shape Changes in Azobenzene Functionalized Polymers Prepared by Ring-Opening Metathesis Polymerization. *Macromolecules* **40,** 1838–1842 (2007).

95. Kim, H.-K. *et al.* Photomechanical Switching Behavior of Semi-Interpenetrating Polymer Network Consisting of Azobenzene-Carrying Crosslinked Poly(vinyl ether) and Polycarbonate. *Macromol. Rapid Commun.* **26,** 1032–1036 (2005).

96. Kusano, D., Ohshima, R., Hosono, N., Totani, K. & Watanabe, T. Photochemical reaction in azobenzene-containing rigid poly(amide acid) networks. *Polymer* **55,** 5648–5655 (2014).

97. Reed, J. P. *et al.* Large-Area Three-Dimensional Molecular Ordering of a Polymer Brush by One-Step Processing. *Science* **330,** 805–808 (2010).

98. Sun, W., Zhou, S., You, B. & Wu, L. Polymer brush-functionalized surfaces with unique reversible double-stimulus responsive wettability. *J. Mater. Chem. A* **1,** 10646–10654 (2013).

99. Hu, X., Zhao, X., Gan, L. H. & Xia, X. Synthesis, characterization, and photochromic properties of PMMA functionalized with 4,4'-diacryloyloxyazobenzene. *J. Appl. Polym. Sci.* **83,** 1061–1068 (2002).

100. Ravi, P. *et al.* New water soluble azobenzene-containing diblock copolymers: synthesis and aggregation behavior. *Polymer* **46,** 137–146 (2005).

101. Micheletto, R. *et al.* Real time observation of trans–cis isomerization on azobenzene SAM induced by optical near field enhancement. *Appl. Surf. Sci.* **228,** 265–270 (2004).

102. Zhang, J., Ma, W., He, X.-P. & Tian, H. Taking Orders from Light: Photo-Switchable Working/Inactive Smart Surfaces for Protein and Cell Adhesion. *ACS Appl. Mater. Interfaces* **9,** 8498–8507 (2017).

103. Gu, R. *et al.* Photocontrolled micellar aggregation of amphiphilic DNA-azobenzene conjugates. *Colloids Surf. B Biointerfaces* **135,** 126–132 (2015).

104. Moldt, T. *et al.* Tailoring the Properties of Surface-Immobilized Azobenzenes by Monolayer Dilution and Surface Curvature. *Langmuir* **31,** 1048–1057 (2015).

105. Zhou, J. & Ritter, H. Cyclodextrin functionalized polymers as drug delivery systems. *Polym. Chem.* **1,** 1552–1559 (2010).

106. Sambasevam, K., Mohamad, S., Sarih, N. & Ismail, N. Synthesis and Characterization of the Inclusion Complex of β-cyclodextrin and Azomethine. *Int. J. Mol. Sci.* **14,** 3671–3682 (2013).

107. Harada, A. & Takashima, Y. Macromolecular Recognition and Macroscopic Interactions by Cyclodextrins. *Chem. Rec.* **13,** 420–431 (2013).

108. Harada, A., Takashima, Y. & Nakahata, M. Supramolecular Polymeric Materials via Cyclodextrin–Guest Interactions. *Acc. Chem. Res.* **47,** 2128–2140 (2014).

109. Luo, C. *et al.* Light-triggered reversible solubility of α-cyclodextrin and azobenzene moiety complexes in PDMAA-co-PAPA via molecular recognition. *J. Appl. Polym. Sci.* **107,** 2118–2125 (2008).

110. Yuan, W., Shen, J. & Guo, W. Thermoresponse and light-induced reversible self-assembly/disassembly of supra-amphiphiles from azobenzene- and β-cyclodextrin-containing copolymers. *Mater. Lett.* **134,** 259–262 (2014).

111. Zheng, X., Wang, D., Shuai, Z. & Zhang, X. Molecular Dynamics Simulations of the Supramolecular Assembly between an Azobenzene-Containing Surfactant and α-Cyclodextrin: Role of Photoisomerization. *J. Phys. Chem. B* **116,** 823–832 (2012).

112. Bian, Q., Wang, W., Wang, S. & Wang, G. Light-Triggered Specific Cancer Cell Release from Cyclodextrin/Azobenzene and Aptamer-Modified Substrate. *ACS Appl. Mater. Interfaces* **8,** 27360–27367 (2016).

113. Dong, Z.-Q. *et al.* Photoreversible Polymer–Surfactant Micelles Using the Molecular Recognition of α-Cyclodextrin. *Langmuir* **29,** 3188–3194 (2013).

114. Mori, T., Dong, T., Yazawa, K. & Inoue, Y. Preparation of Highly Transparent and Thermally Stable Films ofα-Cyclodextrin/Polymer Inclusion Complexes. *Macromol. Rapid Commun.* **28,** 2095–2099 (2007).

115. Meng, H. *et al.* Autonomous in Vitro Anticancer Drug Release from Mesoporous Silica Nanoparticles by pH-Sensitive Nanovalves. *J. Am. Chem. Soc.* **132,** 12690–12697 (2010).

116. Moore, S. & Stein, W. H. Photometric Ninhydrin Method for Use in the Chromatography of Amino Acids. *J Biol Chem* 367–388 (1948).

117. Gottlieb, H. E., Kotlyar, V. & Nudelman, A. NMR Chemical Shifts of Common Laboratory Solvents as Trace Impurities. *J. Org. Chem.* **62,** 7512–7515 (1997).

118. White, A. J. & Filisko, F. E. Tacticity determination of poly(methyl methacrylate) (PMMA) by high-resolution NMR. *J. Polym. Sci. Polym. Lett. Ed.* **20,** 525–529 (1982).

119. Hiemenz, P. C. & Rajagopalan, R. Surface Tension and Contact Angle: Application to Pure Substances. in *Principles of Colloid and Surface Chemistry* 248–296 (Marcel Dekker, Inc., 1997).

120. Wenzel, R. N. Resistance of Solid Surfaces to Wetting by Water. *Ind. Eng. Chem.* **28,** 988–994 (1936).

121. Heide, P. van der. *X-ray Photoelectron Spectroscopy: An introduction to Principles and Practices*. (John Wiley & Sons, 2011).

122. Briggs, D. & Grant, J. T. *Surface Analysis by Auger and X-ray Photoelectron Spectroscopy*. (SurfaceSpectra, 2003).

123. Thermo Scientific XPS: Resources. (2017). Available at: https://xpssimplified.com/resources.php. (Accessed: 27th September 2017)

124. G. Beamson & D. Briggs. *High Resolution XPS of Organic Polymers: The Scienta ESCA300 Database*. (Wiley, 1992).

125. M. C. Biesinger. X-ray Photoelectron Spectroscopy (XPS) Reference Pages. (2015).

126. Owen, G. R., Jackson, J., Chehroudi, B., Burt, H. & Brunette, D. M. A PLGA membrane controlling cell behaviour for promoting tissue regeneration. *Biomaterials* **26,** 7447–7456 (2005).

127. Strauss, R. W. *et al.* Changes in intraocular lens surface roughness during cataract surgery assessed by atomic force microscopy. *J. Cataract Refract. Surg.* **38,** 146–154 (2012).

128. He, L., Read, E. S., Armes, S. P. & Adams, D. J. Direct Synthesis of Controlled-Structure Primary Amine-Based Methacrylic Polymers by Living Radical Polymerization. *Macromolecules* **40,** 4429–4438 (2007).

129. Lee, S. B., Russell, A. J. & Matyjaszewski, K. ATRP Synthesis of Amphiphilic Random, Gradient, and Block Copolymers of 2-(Dimethylamino)ethyl Methacrylate and *n* -Butyl Methacrylate in Aqueous Media. *Biomacromolecules* **4,** 1386–1393 (2003).

130. Lad, J., Harrisson, S., Mantovani, G. & M. Haddleton, D. Copper mediated living radical polymerisation: interactions between monomer and catalyst. *Dalton Trans.* **0,** 4175–4180 (2003).

131. Tosh, B. & Routray, C. Study of the Effect of Solvent and Initiator on Grafting Parameters during Homogeneous Grafting of Methyl Methacrylate onto Cellulose. *Chem. Sci. Rev. Lett.* **1,** 120–132 (2012).

132. Thompson, K. L., Read, E. S. & Armes, S. P. Chemical degradation of poly(2-aminoethyl methacrylate). *Polym. Degrad. Stab.* **93,** 1460–1466 (2008).

133. Zhang, Y. *et al.* Thermal hazard analyses for the synthesis of benzoyl peroxide. *J. Loss Prev. Process Ind.* **43,** 35–41 (2016).

134. Madison, S. A. & Carnali, J. O. pH Optimization of Amidation via Carbodiimides. *Ind. Eng. Chem. Res.* **52,** 13547–13555 (2013).

135. Satterthwait, A. C. & Jencks, W. P. The Mechanism of the Aminolysis of Acetate Esters. *J. Am. Chem. Soc.* **96,** 7018–7031 (1974).

136. Kim, J. *et al.* Quantitative analysis of surface amine groups on plasma-polymerized ethylenediamine films using UV–visible spectroscopy compared to chemical derivatization with FT-IR spectroscopy, XPS and TOF-SIMS. *Appl. Surf. Sci.* **253,** 4112–4118 (2007).

137. Read, E. S., Thompson, K. L. & Armes, S. P. Synthesis of well-defined primary amine-based homopolymers and block copolymers and their Michael addition reactions with acrylates and acrylamides. *Polym. Chem.* **1,** 221–230 (2010).

138. Yang, M.-C. & Lin, W.-C. Protein adsorption and platelet adhesion of polysulfone membrane immobilized with chitosan and heparin conjugate. *Polym. Adv. Technol.* **14,** 103–113 (2003).

139. Wells, L. A., Furukawa, S. & Sheardown, H. Photoresponsive PEG-Anthracene Grafted Hyaluronan as a Controlled-Delivery Biomaterial. *Biomacromolecules* **12,** 923–932 (2011).

140. Inomata, K. *et al.* Shape memory behavior of poly(methyl methacrylate)-graft-poly(ethylene glycol) copolymers. *Polymer* **51,** 793–798 (2010).

141. Kynclova, E. *et al.* Novel method for coupling of poly(ethyleneglycol) to carboxylic acid moieties of proteins. *J. Mol. Recognit. JMR* **9,** 644–651 (1996).

142. Harder, P., Grunze, M., Dahint, R., Whitesides, G. M. & Laibinis, P. E. Molecular Conformation in Oligo(ethylene glycol)-Terminated Self-Assembled Monolayers on Gold

and Silver Surfaces Determines Their Ability To Resist Protein Adsorption. *J. Phys. Chem. B* **102,** 426–436 (1998).

143. Suh, K. Y. & Jon, S. Control over Wettability of Polyethylene Glycol Surfaces Using Capillary Lithography. *Langmuir* **21,** 6836–6841 (2005).
144. Hong, S. H. & McHugh, V. M. *Review of polymerization and properties of aminoalkyl acrylates and aminoalkyl methacrylates*. (Chemical Research Development and Engineering Center, 1988).
145. Chai, J., Lu, F., Li, B. & Kwok, D. Y. Wettability interpretation of oxygen plasma modified poly(methyl methacrylate). *Langmuir ACS J. Surf. Colloids* **20,** 10919–10927 (2004).
146. Kolpak, A. M. & Grossman, J. C. Azobenzene-Functionalized Carbon Nanotubes As High-Energy Density Solar Thermal Fuels. *Nano Lett.* **11,** 3156–3162 (2011).
147. Bortolus, P. & Monti, S. cis ↔ trans Photoisomerization of azobenzene-cyclodextrin inclusion complexes. *J. Phys. Chem.* **91,** 5046–5050 (1987).
148. Yamaguchi, H. *et al.* Photoswitchable gel assembly based on molecular recognition. *Nat. Commun.* **3,** 603 1-5 (2012).
149. Rekharsky, M. V. *et al.* Thermodynamic and nuclear magnetic resonance study of the reactions of α-and β-cyclodextrin with acids, aliphatic amines, and cyclic alcohols. *J. Phys. Chem. B* **101,** 87–100 (1997).
150. Wagner, N. & Theato, P. Light-induced wettability changes on polymer surfaces. *Polymer* **55,** 3436–3453 (2014).
151. Barillé, R., Janik, R., Kucharski, S., Eyer, J. & Letournel, F. Photo-responsive polymer with erasable and reconfigurable micro- and nano-patterns: An in vitro study for neuron guidance. *Colloids Surf. B Biointerfaces* **88,** 63–71 (2011).

152. Hirose, T. *et al.* Presence of Neutrophil Extracellular Traps and Citrullinated Histone H3 in the Bloodstream of Critically Ill Patients. *PLOS ONE* **9,** e111755 1-9 (2014).

153. Fuchs, T. A. *et al.* Novel cell death program leads to neutrophil extracellular traps. *J. Cell Biol.* **176,** 231–241 (2007).

154. Skubitz, K. M., Campbell, K. D. & Skubitz, A. P. N. CD66a, CD66b, CD66c, and CD66d each independently stimulate neutrophils. *J. Leukoc. Biol.* **60,** 106–117 (1996).

155. Tanaka, H., Abe, E., Miyaura, C., Shiina, Y. & Suda, T. 1α,25-Dihyroxyvitamin D3 induces differentiation of human promyelocytic leukemia cells (HL-60) into monocyte-macrophages, but not into granulocytes. *Biochem. Biophys. Res. Commun.* **117,** 86–92 (1983).

Appendix A. Surface functionalization of PMMA disks

A.1. X-ray photoelectron spectroscopy (XPS) study of surface elemental composition of rough and smooth PMMA disks

The availability of chemical groups at the surface of rough and smooth PMMA were then analysed using XPS. The smooth disk had higher amounts of polar, hydrophilic groups (C=O and C-O) and decreased hydrophobic (CHx) groups at the surface compared to the rough disks (Table A.1), supporting the contact angle results.

Table A.1: XPS peaks for rough and smoothed PMMA disk reported as Atomic Concentration (At %). Green values increased from the rough to smooth PMMA disk while orange values decreased. (n = 1).

	Rough		Smooth	
	Position	At (%)	Position	At (%)
Na 1s	1071.76	0.15		
O 1s, Si-O			534.5	4.05
O 1s, C-O	533.84	8.68	533.67	9.09
O 1s, C=O	532.29	14.53	532.32	12.48
N 1s	400.05	0.41		
C 1s, C=O	289.05	9.82	289.08	12.66
C 1s, C-O	286.91	10.13	286.87	12.75
C 1s, C-C	285.83	12.69	285.79	16.19
C 1s, CHx	285	41.16	285.01	30.51
Cl 2p1/2	200.25	0.02	201.73	0.02
Cl 2p3/2	198.22	0.04	200.13	0.04
Si 2p, O-Si-O			102.9	0.75
Si 2p O-Si-C	102.29	2.35	102.07	1.46

Based upon these results, smoothed PMMA disks were used for functionalization as smoothed surfaces will provide a more consistent environment for further contact angle analysis and the XPS results suggest there are more ester side chains available for reaction on the smoothed surface.

A.2. Contact angles for functionalized PMMA disks

The following tables contain the static water contact angles for amine- and carboxyl-functionalized PMMA disks and coated coverslips, MMAcoAEM-coated coverslips, and azobenzene-modified surfaces before and after incubation with β-cyclodextrin (β-CD).

Table A.2: Static water contact angles for unmodified and amine (short spacer HMD, long spacer PPG-PEG-PPG) and carboxyl functionalized PMMA disks with standard error. (n = 3).

Reaction Conditions	Contact Angle (°)
Rough	80 ± 2
Smooth	76 ± 1
HMD (a) (pH 11.5, 2 h)	76 ± 1
HMD (b) (pH 11.5, 48 h)	71 ± 1
HMD (c) (pH 12.5, 2 h)	67 ± 4
HMD (d) (pH 12.5, 48 h)	66 ± 2
PPG-PEG-PPG (pH 12.5, 2 h)	72 ± 2
Carboxyl (a) (6N NaOH, 2 h)	50 ± 2
Carboxyl (b) (6N NaOH, 6 h)	42 ± 6

Table A.3: Static water contact angles for PMMA disks before and after incubation in β-cyclodextrin solution with standard error. Unmodified PMMA smooth disks and amine modified disks (short spacer HMD, long spacer PPG-PEG-PPG) were used as controls for azobenzene-modified (AZO) disks. (n = 3).

PMMA Disk	Before Incubation Contact Angle (°)	After Incubation Contact Angle (°)
Smooth Disk	76 ± 1	74 ± 1
HMD	67 ± 4	73 ± 2
HMD (c) + AZO	70 ± 1	74 ± 1
PPG-PEG-PPG	72 ± 2	76 ± 2
PPG-PEG-PPG + AZO	72 ± 2	74 ± 1

Table A.4: Static water contact angles for unmodified, amine-functionalized (short spacer HMD, long spacer PPG-PEG-PPG), and azobenzene-modified (AZO) PMMA-coated coverslips before and after incubation with β-cyclodextrin with standard error. (n = 3).

PMMA Coated Coverslip	Before Incubation Contact Angle (°)	After Incubation Contact Angle (°)
Glass Only	57 ± 2	-
PMMA Coated-Coverslip	75 ± 2	67 ± 2
+ HMD	72 ± 1	71 ± 1
+ HMD+AZO	72 ± 2	74 ± 2
+ PPG-PEG-PPG	69 ± 2	74 ± 1
+ PPG-PEG-PPG+AZO	72 ± 1	65 ± 4

Table A.5: Static water contact angles for unmodified and azobenzene-modified (AZO) MMAcoAEM-coated coverslips before and after incubation in β-cyclodextrin with standard error. (n = 3).

MMAcoAEM-Coated Coverslips	Before Incubation Contact Angle (°)	After Incubation Contact Angle (°)
MMAcoAEM	42 ± 1	43 ± 1
MMAcoAEM + AZO	71 ± 1	75 ± 1

Appendix B. HL-60 cell studies on functionalized PMMA

B.1. Rough vs. smooth topology had minimal effect on cell viability

PMA significantly increased the cell adhesion for each surface, with absorbance increased to 0.30 from 0.080 for TCPS ($p = 0.02$), 0.44 from 0.16 for rough PMMA ($p = 0.05$), and 0.42 from 0.14 for smooth PMMA ($p = 0.009$), shown in Figure B.1. There was no significant difference in the viability of HL-60s without PMA grown on rough ($p = 0.15$) or smooth ($p = 0.02$) PMMA disks compared to TCPS. For samples incubated with PMA, there were significant increases in cell viability for rough ($p = 0.02$) and smooth ($p = 0.03$) PMMA disks to 0.44 or 0.42 respectively from 0.30 for TCPS, but no significant difference in cell viability between rough and smooth PMMA ($p = 0.39$) – however these differences a likely a result of the higher number of cells adhering to samples activated with PMA than on samples without PMA.

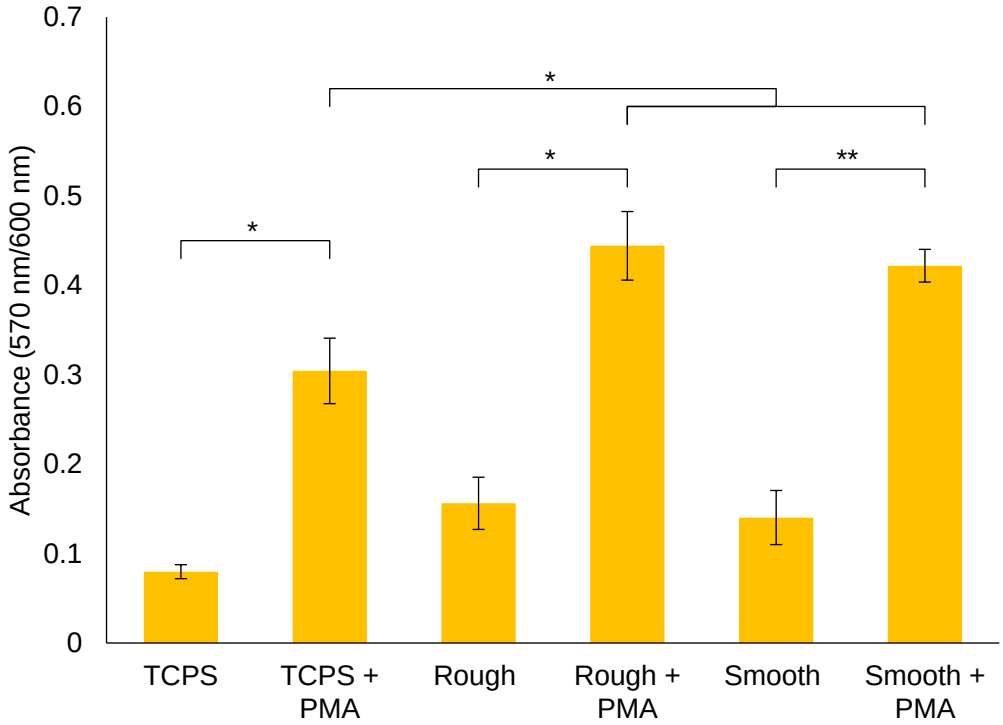

Figure B.1: AlamarBlue® assay results comparing rough and smooth PMMA disks to tissue culture polystyrene (TCPS) with and without PMA activation. ($n = 3$, $*p < 0.05$, $**p < 0.01$).

B.2. Cell viability is higher on amine-functionalized PMMA than TCPS control

A cell viability study was performed for PMMA disks modified with amine (HMD) or carboxyl groups, shown in Figure B.2 and Figure B.3 respectively. There was a significant difference between inactivated and activated cells between TCPS and TCPS + PMA ($p = 0.008$), between NH_2 (c) and NH_2 (c) + PMA ($p = 0.001$), and between NH_2 (d) and NH_2 (d) + PMA ($p = 0.004$). There was a significant increase in absorbance from TCPS to amine modified PMMA disks (c) ($p = 0.01$) and (d) ($p = 0.02$), and from TCPS activated with PMA to activated amine samples (c) ($p = 0.003$) and (d) ($p = 0.02$). Finally, there was no significant difference between NH_2 (c) and NH_2 (d) without ($p = 0.43$) or with ($p = 0.05$) PMA.

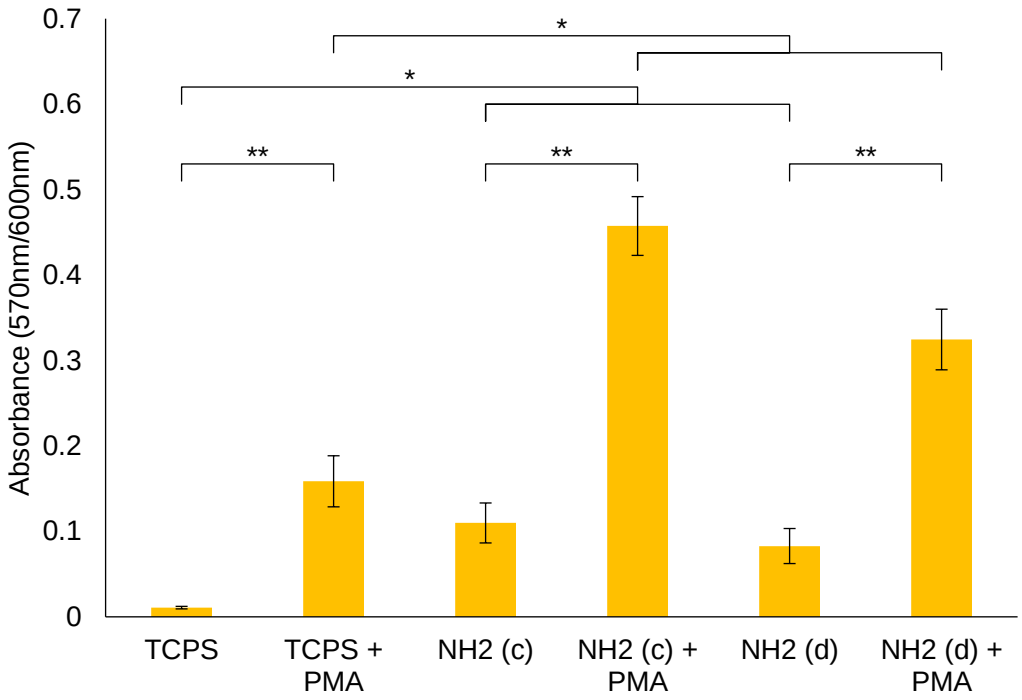

Figure B.2: AlamarBlue® assay results comparing smooth PMMA disks modified with HMD for 2 hours (c) or 48 hours (d) to tissue culture polystyrene (TCPS) with and without PMA activation. ($n = 3$, *$p < 0.05$, ** $p < 0.01$).

B.3. Cell viability is higher on carboxyl-functionalized PMMA than TCPS control

Figure B.3 indicates the significant difference between inactivated and PMA-activated cells growing on TCPS and TCPS + PMA ($p = 0.005$), COOH (a) and COOH (a) + PMA ($p = 0.0002$), and COOH (b) and COOH (b) + PMA ($p = 0.009$). Between TCPS and carboxyl surfaces activated with PMA there were no significant differences for TCPS + PMA and COOH (a) + PMA ($p = 0.47$) or TCPS + PMA and COOH (b) + PMA ($p = 0.92$), unlike the amine-modified surfaces. There was a significant difference between TCPS and COOH (b) ($p = 0.01$) but no significant difference between TCPS and COOH (a) ($p = 0.19$). Finally, there was no significant difference between the COOH (a) and COOH (b) cells without PMA ($p = 0.07$) or with PMA ($p = 0.28$)

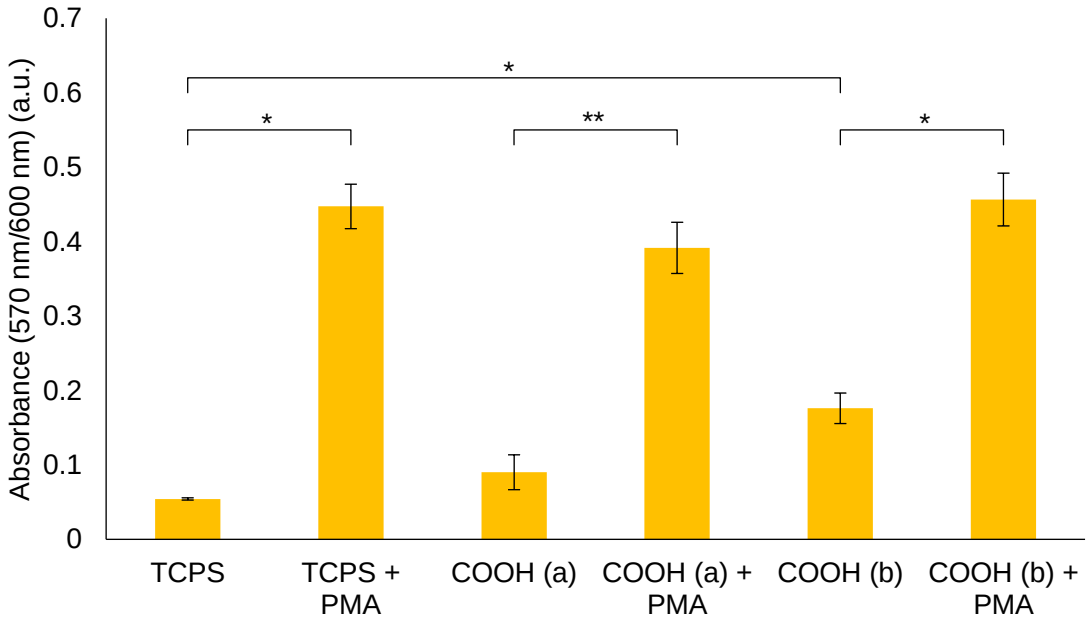

Figure B.3: AlamarBlue® assay results comparing smooth PMMA disks modified with carboxyl groups for 2 hours (a) or 6 hours (b) to tissue culture polystyrene (TCPS) with and without PMA activation. ($n = 3$, $*p < 0.05$, $**p < 0.0005$).